



**UNIVERSIDADE FEDERAL DO PARÁ
INSTITUTO DE GEOCIÊNCIAS
PROGRAMA DE PÓS-GRADUAÇÃO EM GEOLOGIA E GEOQUÍMICA**

DISSERTAÇÃO DE MESTRADO Nº 580

**PALEOAMBIENTE DO GRUPO SERRA GRANDE, BORDA
LESTE DA BACIA DO PARNAÍBA, LOCALIDADE DE
IPUEIRAS, ESTADO DO CEARÁ**

Dissertação apresentada por:

**IVAN ALFREDO ROMERO BARRERA
Orientador: Prof. Dr. Afonso Cesar Rodrigues Nogueira (UFPA)**

**BELÉM-PARÁ
2020**

**Dados Internacionais de Catalogação na Publicação (CIP) de acordo com ISBD
Sistema de Bibliotecas da Universidade Federal do Pará**

Gerada automaticamente pelo módulo Ficat, mediante os dados fornecidos pelo(a) autor(a)

B272p Barrera, Ivan Alfredo Romero

Paleoambiente do Grupo Serra Grande, borda Leste da Bacia do Parnaíba, localidade de Ipueiras, Estado do Ceará. / Ivan Alfredo Romero Barrera. — 2020.

xvi, 58 f.: il. color.

Orientador (a): Prof. Dr. Afonso César Rodrigues Nogueira
Dissertação (Mestrado) - Programa de Pós-Graduação em
Geologia e Geoquímica, Instituto de Geociências, Universidade Federal do Pará, Belém, 2020.

1. Estratigrafía. 2. Sedimentología. 3. Glaciação Siluriana.
4. Bacia de Parnaíba. 5. Grupo Serra Grande. I. Título.

CDD 558.1



**Universidade Federal do Pará
Instituto de Geociências
Programa de Pós-Graduação em Geologia e Geoquímica**

**PALEOAMBIENTE DO GRUPO SERRA GRANDE, BORDA
LESTE DA BACIA DO PARNAÍBA, LOCALIDADE DE
IPUEIRAS, ESTADO DO CEARÁ**

DISSERTAÇÃO APRESENTADA POR:

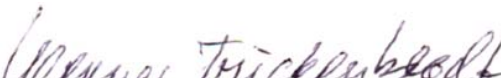
IVAN ALFREDO ROMERO BARRERA

Como requisito parcial à obtenção do Grau de Mestre em Ciências na Área de GEOLOGIA, linha de pesquisa ANÁLISE DE BACIAS SEDIMENTARES.

Data da aprovação: 25 / 04 / 2020

Banca Examinadora:


Prof. Dr. Afonso Cesar R. Nogueira
(Orientador-UFPA)


Prof. Dr. Werner Truckenbrodt
(Membro-UFPA)


Prof. Dr. Francisco Romério A. Junior
(Membro-UFF)

*Dedico esse trabalho a minha família,
por seu apoio incondicional.*

AGRADECIMENTOS

Ao Deus tudo poderoso sempre por tudo, pela saúde e pela oportunidade de me permitir ter novas experiências, conhecer novas pessoas e diferentes locais durante minha vida.

Ao CNPq, PPGG e à Universidade Federal do Pará, pelo suporte financeiro e estrutural durante o desenvolvimento desta pesquisa.

Ao Prof. Dr. Afonso Nogueira, pela amizade, orientação, sugestões, discussões, conselhos e, pela confiança dada para o desenvolvimento desta pesquisa.

Ao laboratório de Microanálises do Instituto de Geociências da Universidade Federal do Pará, nas pessoas do Prof. Dr. Claudio Nery Lamarão, Msc. Gisele Tavares Marques, e a Ana Paula Corrêa pelo auxílio na obtenção das imagens no Microscópio Eletrônico de Varredura (MEV).

Agradeço aos técnicos: Everaldo Cunha (Laboratório de Sedimentologia); Joelma Soares e Bruno Veras (Laboratório de Laminação), pela ajuda e boa disposição.

Aos Profs. Drs. Joelson Soares e José Bandeira, pelas sugestões, discussões e apoio sempre que precisei.

Aos Profs. Drs. Werner Truckenbrodt, Ana Góes e Francisco Abrantes pelas sugestões, comentários construtivos em este documento.

Aos amigos do GSED, Guilherme Raffaeli, Pedro Augusto, Walmir Lima, Hudson Santos, Renato Sol, Luiz Saturnino, Roberto Araújo, Raphael Araújo, Lucas Cunha, Adriana Medina, Renan Fernandes, Alexandre Ribeiro, Andressa Nogueira e Sebastian Gomez, pela amizade e acompanhamento durante o desenvolvimento desta pesquisa.

Às secretárias Cleida Freitas e Joanicy Lopes, pela gentiliza, apoio, atenção e simpatia.

Agradeço especialmente a Adriana Medina pelo carinho e por ser uma revisora constante deste trabalho.

Agradeço aos meus pais, Esperanza Barrera e Abraham Romero, pelo apoio, investimentos e ensinamentos. Ao meu irmão Manuel Romero por sempre caminhar de meu lado.

Em especial, quero agradecer a minha tia Pepa (*in memoriam*), a pessoa que trouxe mais alegria à minha vida com seu sorriso e seu amor.

Agradeço a todos que, direta ou indiretamente, me auxiliaram a iniciar e concluir este trabalho, cujos nomes não caberiam em poucas páginas.

“Recuerda que al poder y sus responsabilidades, que al prestigio y sus deberes, los pulverizará la muerte en un instante. La muerte que no nos deja olvidar que estamos de paso, que la vida es sólo una noche que pasamos en una posada que se encuentra a la vera del camino”.

Facundo Cabral

RESUMO

A transição entre os períodos Ordoviciano e Siluriano na porção oeste do supercontinente Gondwana foi marcada por um longo período glacial, que teve seu máximo no Hirnantiano (~445 Ma). Este evento ocorreu durante um longo período climático de *greenhouse*, no qual o conteúdo de CO₂ na atmosfera era cinco vezes maior que o atual. A migração do supercontinente Gondwana em direção ao Polo Sul foi concomitante com fatores astronômicos tais como mudanças da rotação da terra e diminuição da radiação solar que favoreceu o crescimento dos lençóis de gelo. O final da glaciação foi marcado pelo maior aumento do nível eustático do mar registrado na história da terra, gerando expressivas transgressões marinhas, que iniciaram no Llandovery (~443 Ma) e finalizaram no Ludlow (~423 Ma). Um dos melhores registros destes eventos dentro do contexto de Gondwana Oeste é o Grupo Serra Grande que representa uma sucessão siliciclástica ordoviciano-devoniana presente na Bacia do Parnaíba, nordeste do Brasil. Esta sequência aflorante na borda leste da bacia é dividida em três formações: Ipu, Tianguá e Jaicós. A maioria dos trabalhos prévios sobre este Grupo tem caráter estritamente regional e litoestratigráfico o que não tem permitido determinar os ambientes e sistemas deposicionais calcados em um arcabouço estratigráfico preciso. Este trabalho apresenta novas interpretações dos sistemas deposicionais presentes no registro do Grupo Serra Grande, baseados em análises sedimentológicas e estratigráficas de afloramentos da região de Ipueiras, Estado do Ceará, nordeste do Brasil. A descrição faciologica detalhada desta sucessão siliciclástica teve como objetivo principal propor um modelo deposicional e evolutivo para estes depósitos. Foram definidas sete associações de fácies (AF) representativas de depósitos gerados em sistemas fluviais, glaciais e costeiros. Depósitos de planície fluvial *sheet braided* (AF1), consistem em arenitos grossos e conglomerados com estratificação cruzada tabular e acanalada. Depósitos glaciais (AF2 e AF3) que correspondem a conglomerado maciço, arenito grosso com estratificação cruzada e diamictitos maciços. Diamictito estratificado com clastos caídos foram depositados em ambiente glacio-marinho (AF4). Folhelhos laminados são interpretados como depositados em ambientes marinhos distais (*offshore*) (AF5) depositados durante estágios pós-glaciais. Depósitos deltaicos (AF6) são constituídos por siltito laminado e arenito com estratificação cruzada sigmoidal com ocorrências do icnogênero *Arthrophycus*. Esta sucessão flúvio-glacial-deltaica é sobreposta erosivamente por arenitos com estratificação cruzada acanalada, depositados dentro de uma planície fluvial *channeled braided* (AF7). Esta proposta confirma parcialmente interpretações paleoambientais previas, descartando a presença depósitos

gerados em leques aluviais e *outwash plains*. A interpretação das sequências estratigráficas presentes no Grupo Serra Grande foi refinada usando principalmente a interpretação coerente de superfícies chave e correlacionando os tratos de sistema com a curva global do nível do mar, fornecendo um modelo evolutivo sequencial de terceira ordem mais robusto que inclui três sequências deposicionais. O desenvolvimento de um amplo sistema fluvial (AF1, Formação Ipu) diretamente sobre o embasamento cristalino da bacia, com espessuras de centenas de metros sugere um rio perene provavelmente suprido por regiões montanhosas ao Oeste do Gondwana. Estes depósitos de idade Ordoviciano Médio foram gerados dentro de condições de mar baixo pertencentes à sequência 1, e são truncados por uma expressiva inconformidade que possivelmente removeu os estratos gerados em condições transgressivas e de mar alto. Essa inconformidade produzida pela dinâmica glacial retirou aproximadamente 25 Ma do registro sedimentar da bacia. A segunda sequência iniciou com o avanço das geleiras no Siluriano inferior, a partir da instalação de um *ice-contact fan* (AF2 e AF3, Formação Ipu), em condições de mar baixo. Durante o recuo das geleiras grandes quantidades de agua e detritos foram liberados permitindo a deposição de diamictitos estratificados com presença de clastos caídos (AF4, Formação Ipu). A fase de desgelo culminou no aumento do nível do mar e posterior deposição de folhelhos negros da AF5 (Formação Tianguá), durante o Siluriano médio a tardio. A fase de mar alto no Siluriano tardio é marcada instalação de um sistema deltaico (AF6, Formação Tianguá). No Devoniano inferior uma nova expressiva etapa de descida do nível do mar produziu uma discordância na plataforma concomitante com a progradação de sistemas fluviais entrelaçados (AF7, Formação Jaicós), em condições de mar baixo pertencentes à sequência 3. A reconstituição paleoambiental e paleoclimática do Grupo Serra Grande forneceu elementos sedimentológicos e estratigráficos importantes para o entendimento das fases transgressivas e regressivas pré e pós-glaciais, além de auxiliar na reconstrução paleogeográfica dos lençóis de gelo do Gondwana Oeste durante os períodos Ordoviciano e Siluriano.

Palavras-chave: Gondwana Oeste. Siluriano. Bacia do Parnaíba. Grupo Serra Grande. Glaciação.

ABSTRACT

The transition between the Ordovician and Silurian periods in the western portion of the Gondwana supercontinent was marked by a long glacial period, which had its peak in the Hirnantian (~ 445 Ma). This event occurred during a long greenhouse climatic period, in which the CO₂ content in the atmosphere was five times greater than the current one. The supercontinent Gondwana migration towards the South Pole was concomitant with astronomical factors such as changes in the rotation of the earth and decreased solar radiation that favoured the ice-sheets growth. The end of the glaciation was marked by the most substantial increase in the eustatic sea-level recorded in the earth history, generating significant marine transgressions, which started at Llandovery (~ 443 Ma) and ended at Ludlow (~ 423 Ma). One of the best records of these events within the West Gondwana context is the Serra Grande Group, which represents an Ordovician-Devonian siliciclastic succession present in the Parnaíba Basin, northeastern Brazil. This sequence outcropping on the eastern edge of the basin is divided into three formations: Ipu, Tianguá, and Jaicós. Previously work of this Group has a strictly regional and lithostratigraphic character, which has not allowed determining the depositional environments and systems based on a precise stratigraphic framework. This work presents new interpretations of depositional systems present in the Serra Grande Group record, based on sedimentological and stratigraphic analyses of the outcrops located in the Ipueiras region, Ceará State, Northeast Brazil. The detailed faciological description of this siliciclastic succession had as main objective to propose a depositional and evolutionary model for these deposits. Outcrop-based facies and stratigraphical analysis of this siliciclastic succession indicated fluvial, glacial, and coastal depositional systems grouped on seven facies associations (FA). Deposits of sheet braided plains (AF1), consisting of coarse and conglomerate sandstones with cross-stratification. Glacial deposits (AF2 and AF3) corresponding to massive conglomerate, thick sandstone with cross-stratification and massive diamictites. Stratified diamictite with drop clasts were deposited in a glacial-marine environment (AF4). Laminated black shales (AF5) are interpreted as deposited in offshore settings during post-glacial stages. Deltaic deposits (AF6) consist of laminated siltite and sandstone with sigmoidal cross-stratification and occurrences of the ichnogenus *Arthrophycus*. This fluvial-glacial-deltaic succession is erosively overlaid by sandstones with trough cross-stratification, deposited within a channelled braided plain (AF7). This proposal confirms partially the previous paleoenvironmental interpretation discarding the presence of subaerial alluvial fan and outwash plain deposits for this unit. The

sequence stratigraphy of Serra Grande Group was refined using mainly the coherent interpretation of the key surfaces and comparing the system tracts with the global sea-level curve providing a more robust third-order sequential evolutive model that includes three depositional sequences. The development of an extensive fluvial system (AF1, Ipu Formation) directly over the basin basement, with thicknesses of hundreds of meters, suggests a perennial river probably supplied by mountainous regions to the west of Gondwana. These deposits of middle Ordovician age were generated under low sea conditions belonging to sequence 1, and are truncated by a significant unconformity that possibly removed the transgressive and highstand strata. This unconformity produced by the glacial dynamics removed approximately 25 Ma from the sedimentary record of the basin. The second sequence started with the advance of the ice-sheets in the early Silurian, with the installation of an ice-contact fan (AF2 and AF3, Ipu Formation), in lowstand conditions. During the ice-sheet retreat, large amounts of water and debris were released, allowing the deposition of stratified diamictites with the presence of dropstones (AF4, Ipu Formation). The transgressive phase culminated in an increase in sea level and subsequent deposition of black shales from AF5 (Tianguá Formation), during the middle to late Silurian period. The highstand phase in the late Silurian is marked by the installation of a delta system (AF6, Tianguá Formation). In the early Devonian, an expressive new stage of sea-level fall produced an unconformity on the continental shelf concomitant with the progradation of a braided river system (AF7, Jaicós Formation), under lowstand phase of sequence 3. The Serra Grande Group paleoenvironmental and paleoclimatic reconstruction provided important sedimentological and stratigraphic elements for understanding the pre- and post-glacial transgressive and regressive phases, as well as assisting in the paleogeographic reconstruction of West Gondwana ice-sheets during the Silurian.

Keywords: West Gondwana. Silurian. Parnaíba Basin. Serra Grande Group. Glaciation.

LISTA DE ILUSTRAÇÕES

CAPÍTULO I

- Figura 1.1- Mapa da área de estudo indicando a localização dos afloramentos visitados durante a fase de campo.....2

CAPÍTULO II

- Figura 2.1- Carta litoestratigráfica da Bacia do Parnaíba, em destaque o Grupo Serra Grande.
Fonte: Vaz *et al.* (2007).....8

CAPÍTULO III

- Figure 1- The Parnaíba Basin in northern Brazil and the study area location. A) Simplified geology of the basin. B) Geological map of the Ipueiras district region of Ibiapaba Hill with the locations of visited outcrops. C). Panoramic section of Ibiapaba Hill with indication of a regional unconformity (red line) at the base of the Serra Grande Group (SGG). Geological map at 1:100,000 of the Ipueiras district extracted from the database of the Geological Survey of Brazil (CPRM 2013).....14

- Figure 2- Sedimentary logs and descriptions of facies associations in the Serra Grande Group in the Ipueiras region, eastern Parnaíba Basin, northeastern Brazil. Note the glacial surface erosion (GSE) on the basis of FA2.19

- Figure 3- Faciological aspects of FA1. A) Panoramic section depicting the fining-upward cycles (arrows) in the tabular sandstones with cross-bedding. Note a 1.85 m-tall geologist for scale inside the white circle. B) Detail of the incipient fining-upward pattern in FA1, represented by white triangles. C). Imbricated clasts observed in the bottom of an incipient fining-upward cycle. D) Cross-stratified sandstone facies with coarse particle size segregation in the foresets.....21

- Figure 4- Faciological aspects of FA2. A) and B) Contact between massive diamictite (FA3) and conglomerate interbedded with sandstone exhibiting normal gradation, megaripple and low-angle cross-bedding. C) Detail of A) showing megaripple bedding with well-defined limits, graded beds and cross-bedding. D) and E) Cross-laminated fine sandstone (Cl) alternating with even parallel stratified conglomerate (C); note the granulometric segregation in the foresets with clasts following the cross-strata and load casts (arrows). F) Megaclast of banded gneiss (the scale is a pencil of 15 cm).....24
- Figure 5- Deformational features in the contact zone between FA2 and FA3. A) Megarippled bedded sandstone (mb) underlaid by distinct intervals of diamictite (1-4) with dropstone (dp) and load cast (lc) features. Note in A) the fining-upward cycle (1) overlying megarippled bedded sandstone and underlain by massive diamictite intervals. F) and G) Contact between massive diamictite of FA3 overlying siltstone and sandstone of FA2 with convolute bedding and microfaults. E) and F) Details of the contact between massive pebbly sandstone and conglomerate with microfault and convolute bedding.....25
- Figure 6- Textural and faciological aspects of FA3 (A to E) and FA4 (F-G). A) and B) Massive diamictite with angular to subrounded clasts of wide compositional variety (m-metamorphic, q-quartz, v-volcanic, g-granite, s-sedimentary). C) Petrographic aspect of massive diamictite. D) and E) Scanning electron microscopy (SEM) images showing microtextures observed on quartz sand grain surfaces that include conchoidal fracture (1), striated surface (2), crushing surface (3), and smoothed surface (4). F) Stratified diamictite. G) Dropstones deforming basal strata in diamictite.....27
- Figure 7- Faciological aspects of FA4, FA5 and FA6. A) Contact between the laminated to massive black shale facies association (FA5) and the cross-stratified sandstones and laminated siltstone facies association (FA6). B) Detail of A), exhibiting dropstone (arrows) and dumpstone (rectangle) structures present in FA4. C) Detail of B), showing the composition of the diamictites that compose the dumpstone structures. D) and E) Details of two different types of ichnotaxon *Arthrophycus* identified on FA6.....30

Figure 8- Faciological aspects of cross-stratified sandstones and laminated siltstones facies association (FA6). A), B) and C) Panoramic sections showing coarsening-upward cycles with lobe geometry formed by sigmoidal cross-strata and laminated siltstone interbedded with cross-laminated sandstone. D) Detail of A with subcritical climbing-ripple cross-lamination. E) and F) General view and close-up of water-escape structures identified in laminated fine-grained sandstone; note the down-warped laminations deforming low-angle cross-stratification.....	32
Figure 9- Faciological aspects of FA7. A) Lenticular geometry. B) Trough cross-stratification. C) Plane view of trough cross-stratification dipping to the NW.....	34
Figure 10- Simplified depositional model for the glacial record in the Serra Grande Group. A) During the ice sheet advance, deposits of massive diamicton by the ablation process were reworked by currents with migration of bedforms under partial suspension debris. B) Glacial retreat allowed the release of a large volume of meltwaters concomitant with gradual sea-level rise. In this phase, stratified diamictons were underlain by deposits of organic-rich muds initially influenced by ice rafted debris coming from icebergs. The glacially influenced sea-level rise led to progressive long-term transgression.....	37

Figure 11- Stratigraphic analysis of the Ordovician-Devonian Serra Grande Group in the western Parnaíba Basin. Age, stacking patterns, paleoenvironment, and glacio-eustatic cycles are compared using the proposals of Assis *et al.* (2019), Barrera *et al.* (2018) and this work. Glacial deposits are used as stratigraphic markers to organize the age of succession based on paleontological data. The high-resolution stratigraphic data presented in this work allow correlations with the global relative sea-level curve for the lower Paleozoic and the age calibration of lithostratigraphic and systems tracts such as 1) the lower part of the Serra Grande Group previously interpreted as Late Ordovician and now repositioned in the Middle Ordovician; 2) the ice age previously considered Hirnantian and changed to Llandoverian according to the age obtained in the Amazona and Paraná basins (Melo 1997, Melo & Steemans 1997, Mizusaki *et al.* 2002); and 3) the systems tracts and the nondeposition or erosive intervals (“a” and “b”) tentatively inferred following the curve inflection. Abbreviations: Lst, Lowstand systems tract; Fsst, Falling stage systems tract; Tst, Transgressive systems tract; Hst, Highstand systems tract; GIA, Glacio-isostatic adjustment; AF, Alluvial fan; GF, Glacio-fluvial.39

Figure 12- Sequential evolution of the Serra Grande Group in the eastern Parnaíba Basin. A) Middle Ordovician: the lowstand phase promoted the development of sheet braided deposits of Seq1 coming from southeastern Gondwana. B) Middle to Late Ordovician: the maximum glaciation promoted an extensive lowstand and massive erosion of substrate, totally removing the highstand and transgressive systems tracts of Seq1. C) Early Silurian: the lowstand phase of Seq2 was related to the advance of ice sheets in marginal areas of the basin, causing the deposition of ablation diamicton. The transgressive systems tract started during ice retreat and shedding of icebergs with pronounced deposition by ice rafted debris. D) Middle to late Silurian: the progressive sea-level rise and maximum flooding were accompanied by organic matter-rich mud in offshore settings, and subsequent progradation of a deltaic deposit marked the highstand phase. E) Early Devonian: an extensive sea-level fall renewed the continental drainage with the formation of a braided plain.....44

SUMÁRIO

DEDICATÓRIA	iv
AGRADECIMENTOS	vi
RESUMO.....	viii
ABSTRACT	x
LISTA DE ILUSTRAÇÕES.....	xi
CAPITULO I INTRODUÇÃO.....	1
1.1 APRESENTAÇÃO.....	1
1.2 ARÉA DE ESTUDO	2
1.3 OBJETIVOS.....	3
1.4 MATERIAIS E MÉTODOS.....	3
1.4.1 Análise de fácies e estratigráfica	3
1.4.2 Análises petrográficas e de validação para deformações glaciotectônicas	4
CAPITULO II CONTEXTO GEOLOGICO.....	5
2.1 GLACIAÇÃO ORDOVICIANA-SILURIANA.....	5
2.2 REGISTRO GLACIAL SILURIANO EM GONDWANA OESTE	6
2.3 BACIA DO PARNAÍBA	7
2.4 GRUPO SERRA GRANDE	8
2.4.1 Formação Ipu.....	8
2.4.2 Formação Tianguá.....	9
2.4.3 FORMAÇÃO JAICÓS	10
CAPITULO III THE SILURIAN GLACIATION ON THE EASTERN PARNAIBA BASIN, BRAZIL: PALEOENVIRONMENT, SEQUENCE STRATIGRAPHIC AND INSIGHTS FOR THE EVOLUTION AND PALEOGEOGRAPHY OF WEST GONDWANA	12
3.1 INTRODUCTION	13
3.2 GEOLOGICAL SETTING.....	15
3.2.1 The Parnaíba Basin	15
3.2.2 The Serra Grande Group.....	15
3.2.3 Age constrains	16
3.3 METHODS.....	17

3.4 FACIES ANALYSIS.....	18
3.4.1 Tabular cross-bedded conglomerate and sandstone facies association (FA1)	18
3.4.2 Sandstone with cross-stratification and megaripple bedding facies association (FA2)	21
3.4.3 Massive diamictites facies association (FA3).....	23
3.4.4 Stratified diamictites facies association (FA4)	28
3.4.5 Laminated to massive Black shales facies association (FA5).....	29
3.4.6 Cross-stratified sandstones and laminated siltstones facies association (FA6).....	30
3.4.7 Trough cross-stratified sandstones facies association (FA7)	33
3.5 FACIES MODEL	35
3.6 SEQUENCE STRATIGRAPHY	37
3.6.1 Parasequences	40
3.6.2 Discontinuity surfaces	41
3.6.3 System tracts and depositional sequences	42
3.7 ORDOVICIAN-SILURIAN ICE AGE IN WESTERN GONDWANA	43
3.8 CONCLUSION	45
CAPÍTULO IV CONSIDERAÇÕES FINAIS	47
REFERÊNCIAS	49

CAPÍTULO I INTRODUÇÃO

1.1 APRESENTAÇÃO

O período Siluriano é o período de mais curta duração da era paleozoica (~24 Ma), dentro deste intervalo de tempo aconteceram grandes variações de temperatura a nível global, assim como grandes variações no nível eustático do mar (Melchin *et al.* 2012, Munnecke *et al.* 2010, Scotese 2016). Na Bacia do Parnaíba estas variações climáticas e do nível do mar, estão documentadas principalmente nos depósitos siliciclásticos do Grupo Serra Grande. Este registro é constituído por sucessões pré-glaciais (porção inferior da Formação Ipu) (Caputo & Lima 1984), glaciais (porção superior da Formação Ipu) (Caputo 1984, Caputo & Lima 1984, Grahn *et al.* 2005, Kegel 1953), pós-glaciais-transgressivas (Formação Tianguá) (Caputo 1984, Caputo & Lima 1984, Carozzi *et al.* 1975, Vaz *et al.* 2007) e depósitos relacionados à queda acelerada do nível do mar (Formação Jaicós) (Caputo, 1984, Caputo & Lima 1984, Góes *et al.* 1992, Vaz *et al.* 2007).

Importantes discussões acerca dos modelos deposicionais, idades e correlações dos registros glaciais depositados no Gondwana Oeste durante o Paleozoico Inferior, tem tomado grande relevância em reconstruções dos modelos paleoambientais e paleogeográficos. Características como a natureza glacial definida para diamictitos depositados durante o Siluriano Inferior, além do diacronismo a escala continental destes depósitos, auxiliaram em reconstruções paleogeográficas como evidências do deslocamento do supercontinente através da zona polar (Díaz-Martínez & Grahn 2006). Durante as últimas décadas, muitos trabalhos tiveram como objetivo principal propor um posicionamento estratigráfico do Grupo Serra Grande, estes estudos estiveram baseados, majoritariamente em interpretações paleontológicas, impulsados principalmente pela indústria dos hidrocarbonetos (Caputo & Lima 1984, Grahn *et al.* 2005, Le Hérissé *et al.* 2001). Análises realizadas na Formação Tianguá, baseadas na identificação de palinomorfos e graptólitos (*Climacograptus cf. scalaris scalaris*) permitiram definir uma idade Llandovery Médio (Grahn *et al.* 2005, Le Hérissé *et al.* 2001). Estes dados representam a melhor idade definida dentro do Grupo Serra Grande para seu posicionamento estratigráfico.

A sequência Ordovíciana-Devoniana da Bacia do Parnaíba apesar de ter sido alvo de diferentes trabalhos puramente litoestratigráficos de caráter regional nas últimas décadas, em decorrência principalmente da exploração de óleo e gás pela PETROBRAS (Góes *et al.* 1990), carece de estudos sedimentológicos e faciológicos de detalhe que permitam um melhor

entendimento desses depósitos. Neste sentido, este trabalho utilizou análises de fácies e estratigrafia de alta resolução, para determinar os paleoambientes e evolução dos sistemas deposicionais presentes, assim como as implicações paleogeográficas e paleoclimáticas destes depósitos no contexto do Gondwana Oeste.

1.2 ARÉA DE ESTUDO

A área de estudo encontra-se localizada ao nordeste do Brasil, oeste do Estado do Ceará, na Mesorregião do Noroeste Cearense e na Microrregião de Ipu, em proximidades do município de Ipueiras (Figura 1.1). Os afloramentos ocorrem na borda morfológica leste da Bacia do Parnaíba, onde foram realizadas descrições em exposições do tipo corte de estrada presentes na rodovia CE-257 desde a cidade de Ipueiras até a Serra de Ibiapaba, em uma seção contínua do Grupo Serra Grande.

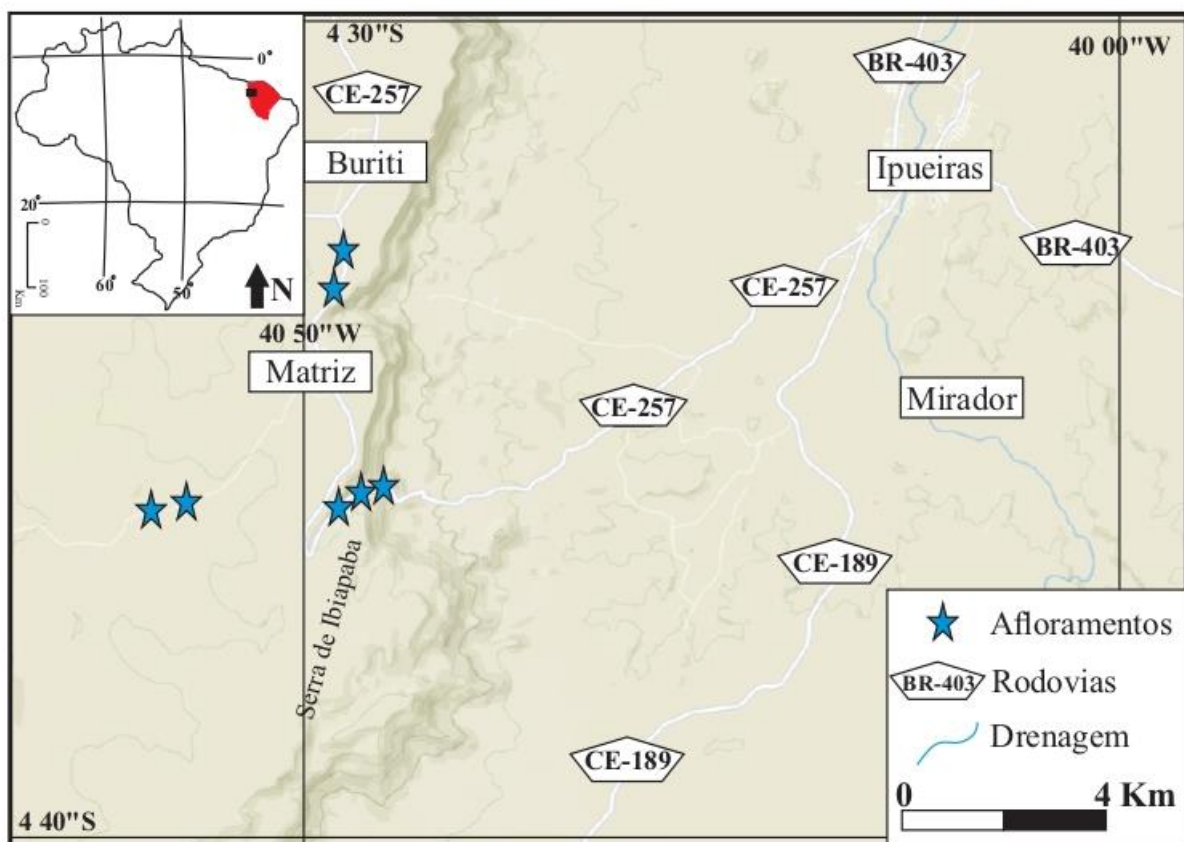


Figura 1.1- Mapa da área de estudo indicando a localização dos afloramentos visitados durante a fase de campo.

1.3 OBJETIVOS

O presente trabalho de mestrado teve como objetivo principal analisar os depósitos siliciclásticos da Sequência Ordoviciana-Devoniana da Bacia do Parnaíba, representado pelas

formações Ipu, Tianguá e Jaicós, com o intuito de melhorar a compreensão da história deposicional da Bacia do Parnaíba durante o Paleozoico Inferior. Para alcançar estas metas, foram cumpridos os seguintes objetivos específicos: i) Estudar os depósitos do Grupo Serra Grande, com o intuito de possibilitar sua reconstituição paleoambiental e paleogeográfica; ii) Inserir a sequência Ordoviciano-Devoniana da Bacia do Parnaíba nos eventos globais do início do Paleozoico que afetaram Gondwana Oeste.

1.4 MATERIAIS E MÉTODOS

Com o fim de alcançar os objetivos anteriormente propostos foram realizados estudos sedimentológicos e estratigráficos de detalhe dos depósitos pertencentes ao Grupo Serra Grande, baseado em dados de afloramento, onde foram empregadas técnicas agrupadas em dois grupos principais: i) análise de fácies e estratigráficas, e, ii) análises petrográficas e de validação para deformações glaciotectônicas.

1.4.1 Análise de fácies e estratigráfica

A análise de fácies foi realizada de acordo com as técnicas propostas por Walker (1992). Os procedimentos consistiram na individualização e descrição das fácies por meio da caracterização e descrição de parâmetros como a composição, geometria, texturas e estruturas sedimentares, conteúdo fossilífero, e padrões de paleocorrentes dos corpos sedimentares, aliado ao entendimento dos processos sedimentares responsáveis pela gênese das fácies. Dessa forma, as fácies contemporâneas e geneticamente relacionadas foram agrupadas em associações de fácies, proporcionando a interpretação paleoambiental e dos sistemas deposicionais.

Para a composição do arcabouço estratigráfico foi utilizada a análise de sequências estratigráficas de alta-resolução, baseada na interpretação de superfícies chave e mudanças de fácies e associações de fácies influenciadas por subida e descida do nível relativo do mar de alta magnitude e/ou taxa de suprimento sedimentar, refletido no *trend* progradante ou retrogradante dos depósitos (Ghienne *et al.* 2007, Le Heron *et al.* 2012, Zecchin & Catuneanu 2013, Zecchin *et al.* 2015). As análises de fácies e estratigráficas foram auxiliadas por perfis verticais, bem como por seções esquemáticas e panorâmicas obtidas a partir de fotomosaicos dos afloramentos para o entendimento geométrico e variações laterais e verticais das fácies (Wizevici 1991).

1.4.2 Análises petrográficas para validação de deformações glaciotectônicas

Com o objetivo de atestar a presença de deformações produzidas por glaciotectônica dentro do registro glacial do Grupo Serra Grande foi realizada a coleta sistemática de amostras seguindo principalmente a individualização das fácies. As características mesoscópicas foram testadas em lajes polidas, enquanto as feições microscópicas foram avaliadas em 12 lâminas polidas, confeccionadas no laboratório de laminação da UFPA. Estas seções foram descritas no Laboratório de Petrografia do Grupo de Análises de bacias Sedimentares da Amazônia – GSED da UFPA, baseado na proposta de Menzies *et al.* (2016), para descrições micromorfológicas de depósitos glaciais. Com o intuito de identificar microtexturas presentes nas superfícies de grãos de quartzo extraídos das amostras de diamictitos glaciais, estes foram revestidos com ouro e fotografados usando elétrons secundários no Microscópico Eletrônico de Varredura modelo Zeiss LEO-1430, pertencente ao Laboratório de Microscopia Eletrônica de Varredura da UFPA (LABMEV-UFPA).

CAPITULO II CONTEXTO GEOLÓGICO

2.1 GLACIAÇÃO ORDOVICIANA-SILURIANA

Durante a passagem dos períodos Ordoviciano e Siluriano, um longo período glacial afetou grande parte da porção oeste do supercontinente Gondwana (Ghienne 2003). Os registros desse evento podem ser observados em rochas de idade ordovicianas no continente africano (Deynoux *et al.* 1985, Ghienne 2003, McDougall & Martin 2000) e rochas de idade siluriana no continente sul-americano (Díaz-Martínez & Grahn 2006, Grahn & Caputo 1992). Este evento glacial ocorreu durante um longo período climático de estufa (*greenhouse*) e foi o produto da deriva do supercontinente para baixas latitudes (Brenchley *et al.* 1994, Brenchley *et al.* 2003). O evento glacial iniciou aproximadamente no Hirnantiano (~ 445 Ma) (Ghienne 2007), e finalizou com a deriva do supercontinente em direção ao norte no Siluriano inferior (Frakes *et al.* 1992). O fim deste longo período glacial forneceu um cenário no qual ocorreram grandes eventos transgressivos que marcaram a história do período Siluriano (Munnecke *et al.* 2010).

Os eventos transgressivos mencionados acima representam o aumento mais significativo do nível eustático do mar registrado na história da Terra, com magnitudes variando de algumas dezenas a no máximo 70 metros (Brenchley *et al.* 1994, Munnecke *et al.* 2010). Haq & Schutter (2008), definiram esse episódio como um aumento do nível do mar em longo prazo, que iniciou no Llandovery (~ 443 Ma) e finalizou no Ludlow (~ 423 Ma). Adicionalmente, durante esse contínuo aumento do nível do mar, sete eventos transgressivos menores foram registrados em Gondwana (Johnson 1996). As flutuações do nível do mar registradas no Fanerozóico a nível global foram controladas principalmente pela dinâmica interna da Terra, que refletiu principalmente no desenvolvimento e na tectônica das placas (Larson 1991, Müller *et al.* 2008, Wagreich *et al.* 2014). Em estágios em que há um rápido crescimento da crosta marinha, um aumento no volume das dorsais mesoceanicas produz um deslocamento da água e um incremento do nível do mar nas costas continentais (Stronge *et al.* 2005). Posteriormente, ao final do período Siluriano, houve uma acelerada queda no nível do mar, atribuída a um atraso no ciclo tectono-eustático (Johnson 1996). Durante o início do período Devoniano, Gondwana Oeste ainda estava localizado na zona polar (Torsvik & Cocks 2013). No entanto, as condições climáticas eram completamente diferentes das do período Siluriano, a temperatura média global mostrou um aumento sistemático devido ao retorno das condições de efeito estufa (Scotese 2015).

2.2 REGISTRO GLACIAL SILURIANO EM GONDWANA OESTE

Durante o Fanerozóico, grandes eventos climáticos e tectônicos afetaram significativamente a porção oeste do supercontinente Gondwana (Milani & Thomaz Filho 2000). Esses eventos controlaram a morfologia e o início da deposição na maioria das grandes bacias sedimentares no oeste de Gondwana (Milani & Thomaz Filho 2000). As bacias intracratônicas brasileiras compartilham uma similaridade significativa em seu registro sedimentar Paleozoico, devido a um início de deposição contemporâneo como reflexo das estruturas herdadas do ciclo Brasil-Pan-Africano (Milani & Thomaz Filho 2000). Linol *et al.* (2016), com base em reconstruções paleogeográficas, definiram a presença de uma extensa cordilheira na porção central do Gondwana que atuaria como fonte de sedimentos para muitas dessas bacias. O evento glacial siluriano descrito neste trabalho afetou a maioria das bacias sedimentares presentes na plataforma sul-americana, este registro e sua relação temporal serão explicados abaixo.

Na Bacia do Amazonas, este evento está representado principalmente por diamictitos e arenitos foliados, depositados em ambientes subglaciais (Soares 1998). As análises de palinomorfos encontradas nos diamictitos presentes na Formação Nhamundá revelaram uma idade Llandovery-Wenlock para depósitos glaciais na bacia amazônica (Melo 1997, Melo & Steemans 1997). Na Bacia do Paraná, o registro glacial presente na Formação Iapó, representado principalmente por diamictitos, conglomerados e siltitos (Adôrno 2014), interpretado como depositado a partir de geleiras em águas marinhas rasas (Assine *et al.* 1998). Adôrno (2014) descreve a interfase entre a Formação Iapó e a Formação Vila Maria como transicional, encontrando similaridades nas faunas fósseis presentes em ambas as formações. Datações absolutas de Rb-Sr realizadas em folhelhos negros basais da Formação Vila Maria indica uma idade de $435,9 \pm 7,8$ Ma, para esses depósitos (Mizusaki *et al.* 2002).

Durante o Paleozóico Inferior, a Bacia Peru-Bolívia representava grande parte da zona marginal oeste do supercontinente Gondwana (Díaz-Martínez & Grahn 2006). Com ampla distribuição lateral, esta bacia estava presente em muitos países da América do Sul (Peru, Bolívia, Colômbia, Venezuela, Argentina e parte mais ocidental do Brasil) (Díaz-Martínez & Grahn 2006). Durante o Paleozoico Inferior esta bacia poderia estar conectada ao norte com a Bacia do Amazonas e ao sul com a Bacia do Paraná (Díaz-Martínez & Grahn 2006). Atualmente, registros glaciais do Paleozoico inferior foram identificados nessa extensa bacia sedimentar em países como Peru, Bolívia e Argentina, representados pelas formações San

Gaban, Cancañiri e Zapla (Díaz-Martínez *et al.* 2001, Díaz-Martínez & Grahn 2006). Esses registros foram interpretados como inicialmente depositados por geleiras aterradas e posteriormente resedimentados por fluxos gravitacionais, que transportaram esses sedimentos para as porções mais profundas da bacia (Díaz-Martínez 1997a, 1998, Rodrigo *et al.* 1977). Com base em uma análise da fauna de quitinozoários presente no registro glacial, Grahn & Gutiérrez (2001) e Díaz-Martínez & Grahn (2006) definiram uma idade de Llandovery (Aeronian-Telychiano) para as formações Zapla e Cancañiri.

O siluriano é um período marcado pela presença de grandes eventos transgressivos, registrados globalmente em espessas camadas de *black shales* com alto conteúdo fossilífero que são de grande importância em termos de correlação (Melchin *et al.* 2012). Na Bacia do Parnaíba, esse evento registrado na Formação Tianguá, e seus equivalentes nas bacias intracratônicas brasileiras são a Formação Pitinga, na Bacia Amazonas, e a Formação Vila Maria, na Bacia do Paraná. Adicionalmente, registros deste evento podem ser observados na Plataforma Sul-Americana, presentes nas formações Ananea no Peru, Kirusillas na Bolívia e Lipeón e Chachipunco na Argentina.

2.3 BACIA DO PARNAÍBA

A Bacia do Parnaíba, é classificada como uma bacia paleozoica do tipo intra-cratônica, localizada ao norte da Plataforma Sul Americana, nordeste do Brasil, com área dimensionada em aproximadamente 600.000 Km² e pode atingir de 3.4 a 3.5 km de espessura nos seus depocentros (Caputo 1984, Daly *et al.* 2014, Vaz *et al.* 2007). Esta bacia, definida como do tipo *sag* (Daly *et al.* 2014), apresenta baixas e localizadas taxas de subsidência, controladas por ciclos orogênicos que não estão relacionados a limites de placas tectônicas (Daly *et al.* 2014). A origem e evolução da Bacia do Parnaíba estão relacionados, principalmente, a eventos tectonomagnéticos (Daly *et al.* 2014), que produziram o início da sedimentação durante o Paleozoico a partir de uma depressão Ordoviciano, provocada por ajustes isostáticos e resfriamento após a fusão de Gondwana (Brito Neves *et al.* 1984, De Castro *et al.* 2014). O embasamento da bacia está representado principalmente por rochas ígneas, metamórficas e sedimentares, com idades que vão desde o Arqueano até o Ordoviciano, formados e/ou retrabalhadas durante o Ciclo Brasiliano (Vaz *et al.* 2007). Três diferentes domínios compõem o embasamento da bacia, denominados, bloco Amazônico/Araguaia, bloco Parnaíba e bloco Borborema (Daly *et al.* 2014), junto com um sistema de bacias precursoras pré-silurianas, Riachão e Jaibaras (De Castro *et al.* 2014, Porto *et al.* 2018). A bacia Riacho é uma bacia de

tipo *foreland* de idade Ediacarano-Cambriano inferior, com uma espessura máxima de 1 km, sua origem está relacionada à tectônica Neoproterozóica tardia (Porto *et al.*, 2018). Enquanto a Bacia do Jaibaras de idade Cambro-Ordoviciano, foi gerada a partir de *riffs* produzidos pela reativação de antigas zonas de cisalhamento associadas ao Lineamento Trasnsbrasiliano NE-SW, produzido durante a orogenia Brasileira-Pan-Africana (Oliveira & Mohriak 2003). Durante o Paleozoico inferior sobre o embasamento definido, teve lugar o desenvolvimento de uma grande superfície erosiva denominada inconformidade pré-Siluriana, que representa a transição do embasamento ao preenchimento sedimentar da bacia do Parnaíba (Vaz *et al.* 2007, Daly *et al.* 2014, Porto *et al.* 2018). Góes & Feijó (1994), separaram a estratigrafia desta bacia em cinco sequências: Sequência Siluriana (Grupo Serra Grande); Sequência Devoniana (Grupo Canindé); Sequência Carbonífero-Triássica (Grupo Balsas); Sequência Jurássica (Grupo Mearim) e Sequência Cretácea (Formações Grajaú, Codó e Itapecuru). No entanto, Vaz *et al.* (2007) dividiram o preenchimento sedimentar da bacia com base em a identificação de descontinuidades regionais, Assim: Sequência Siluriana (Grupo Serra Grande); Sequência MesoDevoniana-EoCarbonífera (Grupo Canindé); Sequência NeoCarbonífera-EoTriássica (Grupo Balsas); Sequência Jurássica (Formação Pastos Bons) e Sequência Cretácea (Formações Corda, Grajaú, Codó e Itapecuru) (Figura 2.1).

2.4 GRUPO SERRA GRANDE

Small (1914) propôs o termo “Série Serra Grande” para englobar uma sucessão sedimentar com uma espessura de até 900 m, composta por calcários, arenitos e conglomerados. Este conceito foi examinado por Kegel (1953), que redefiniu estes limites e propôs o termo Formação Serra Grande, excluindo os calcários dobrados do embasamento, que ocorrem sotopostos e em discordância angular com camadas arenosas. Esta sucessão sedimentar foi elevada à categoria de Grupo por Carozzi *et al.* (1975). Finalmente Caputo & Lima (1984), com base em afloramentos presentes na borda leste da bacia e remanescentes do grupo na bacia de Jatobá, realizaram um posicionamento estratigráfico para o Grupo Serra Grande e separaram este em três formações: Ipu; Tianguá e Jaicós.

2.4.1 Formação Ipu

O termo Ipu foi utilizado por Campbell (1949), para definir a sucessão sedimentar presente na porção basal da escarpa da serra grande. Posteriormente Kegel (1953), descartou este termo ao incluir estes depósitos dentro do que ele descreveu como Formação Serra Grande. Carozzi *et al.* (1975), utilizaram o termo Formação Mirador para diferenciar esta

sucessão sedimentar e inseri-la dentro do contexto do Grupo Serra Grande. Finalmente Caputo & Lima (1984), reassinaram o termo Formação Ipu para os depósitos encontrados na porção basal do Grupo Serra Grande.

A Formação Ipu encontrasse depositada discordantemente sobre as rochas que compõem o embasamento da bacia e exibe um contato transicional com a Formação Tianguá (Caputo & Lima, 1984). Estes depósitos estão compostos principalmente por arenitos, conglomerados, arenitos conglomeráticos e diamictitos, apresentando, na região nordeste da bacia, espessuras de até 300 m (Caputo & Lima 1984). Kegel (1953) descreveu alguns seixos facetados dentro de diamictitos localizados nas porções superiores da Formação Ipu, que tempo depois foram interpretados como de origem glacial. Caputo & Lima (1984), interpretaram os estratos basais da Formação Ipu, como depositados dentro de sistemas fluviais que alimentavam sistemas deltaicos desenvolvidos dentro de ambientes marinhos na porção oeste da bacia.

2.4.2 Formação Tianguá

Rodrigues (1967) utilizou o termo Tianguá para encerrar uma sucessão sedimentar composta por folhelhos negros, siltitos e arenitos finos, descrita em afloramentos dentro da região do município de Tianguá ao nordeste da bacia. Assim o membro Tianguá pertencente à antiga Formação Serra Grande (Kegel 1953), que foi elevado à categoria de formação por Carozzi *et al.* (1975). Caputo & Lima (1984), dividiram a formação em três diferentes membros: (1) folhelho preto a cinza escuro, bioturbado ou laminado e em algumas porções siltosa; (2) arenito fino a médio com intercalações de folhelho; e (3) folhelhos e siltitos intercalados, cinza escuros a verde. A Formação Tianguá tem uma espessura máxima de até 270 metros em subsuperfície e 150 metros medidos em afloramentos na borda leste da bacia (Caputo & Lima 1984). Estes depósitos foram interpretados como depositados dentro de sistemas marinhos rasos e representam grande importância para o posicionamento estratigráfico do Grupo Serra Grande devido à grande diversidade da microfauna presente nestes depósitos (Caputo & Lima 1984, Grahn & Caputo 1992, Grahn *et al.* 2005, Le Hérissé *et al.* 2001).

2.4.3 Formação Jaicós

A Formação Jaicós foi proposta por Plummer (1946), para designar arenitos grossos e conglomerados interpretados em escarpes da serra grande. Carozzi *et al.* (1975), utilizaram o

nome Jaicós para designar a seção sedimentar sobreposta à Formação Tianguá que corresponde à porção superior da Formação Serra Grande proposta por Kegel (1953). Esta unidade está constituída principalmente por arenitos grossos a conglomeráticos, interpretados como depositados dentro de ambientes fluviais e deltaicos, com espessuras máximas de até 400 metros em subsuperfície e 200 metros em superfície (Caputo & Lima 1984, Vaz *et al.* 2007). A Formação Jaicós situa-se concordantemente sobrepondo a Formação Tianguá e na sua porção superior encontrasse limitada por uma discordância regional que a separa da Formação Itaim (Grupo Canindé) (Caputo & Lima 1984).

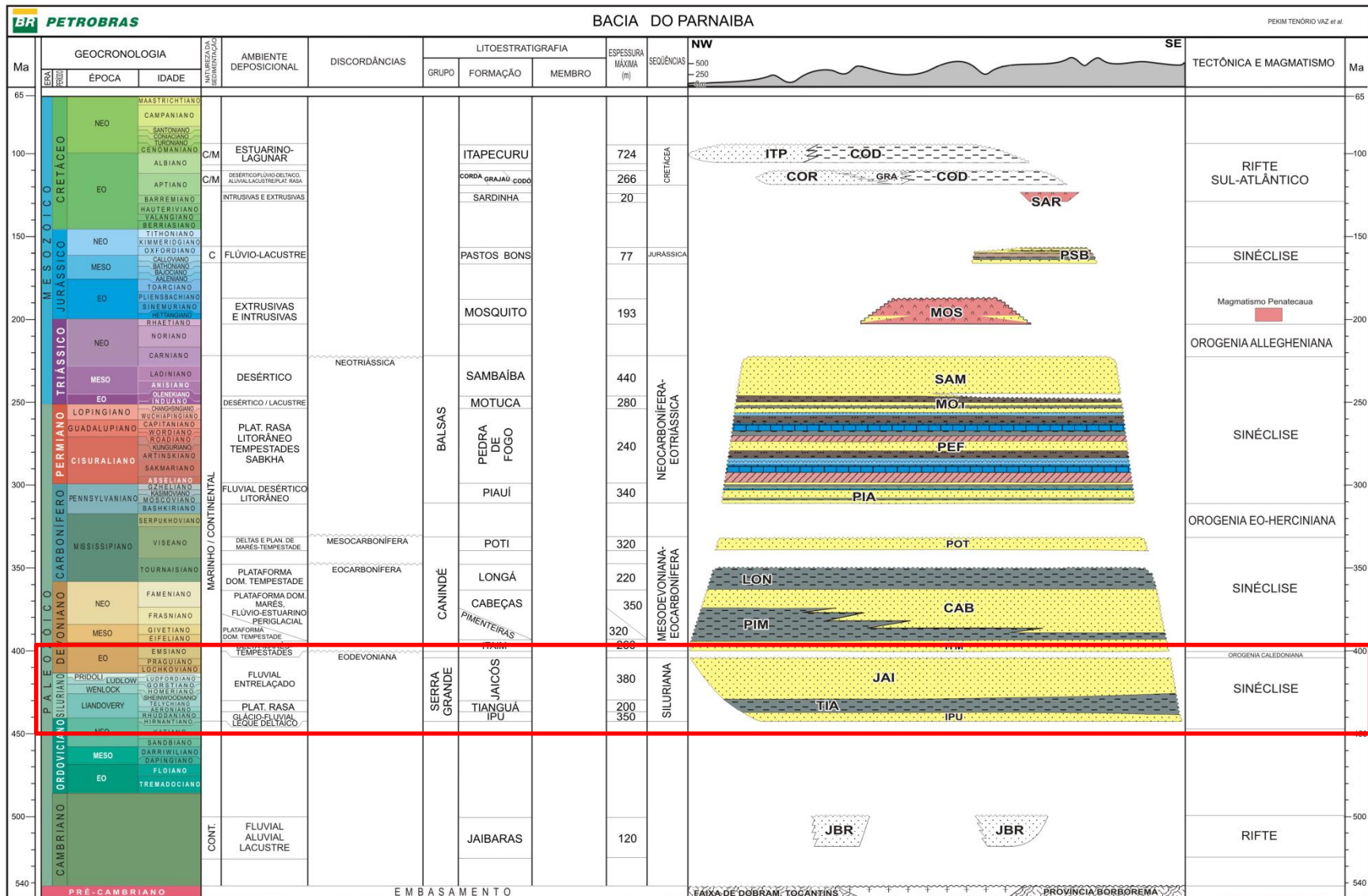


Figura 2.1- Carta litoestratigráfica da Bacia do Parnaíba, em destaque o Grupo Serra Grande. Fonte: Vaz et al. (2007).

CAPÍTULO III THE SILURIAN GLACIATION IN THE EASTERN PARNAÍBA BASIN, BRAZIL: PALEOENVIRONMENT, SEQUENCE STRATIGRAPHY AND INSIGHTS FOR THE EVOLUTION AND PALEOGEOGRAPHY OF WEST GONDWANA

ABSTRACT

Glacial strata are excellent stratigraphic markers in Paleozoic basins worldwide. The eastern Parnaíba Basin in northern Brazil is a highly favorable setting for studying episodes related to the Ordovician-Silurian glaciation. Previous studies in this region led to the recognition of unequivocally glaciogenic sediments associated with pre- and postglacial deposits, favoring the understanding of lower Paleozoic events that occurred in West Gondwana. Outcrop-based facies and stratigraphic analyses of the ~170 m-thick siliciclastic succession of the Serra Grande Group indicate fluvial, glacial, and coastal depositional systems. Seventeen sedimentary facies are grouped into seven facies associations (FAs): FA1, interpreted as intermediary sheet braided plain deposits that consist of tabular cross-bedded coarse-grained sandstones and conglomerates; FA2-FA4, which correspond to subaqueous glacial deposits comprising massive to stratified diamictites, cross-laminated sandstones, diamictites and organic matter-rich black shales with dumpstone and dropstone structures; FA5-FA6, constituting organic matter-rich black shales, fine- to medium-grained sandstones with sigmoidal cross-bedding and occurrences of the ichnotaxon *Arthrophycus* interpreted as delta front deposits; and FA7, composed of medium- to coarse-grained pebbly sandstones interpreted as channelized braided plain deposits. This proposal partially confirms the previous paleoenvironmental interpretation discounting the presence of subaerial alluvial fan and outwash plain deposits for this unit. The sequence stratigraphy of the Serra Grande Group is refined mainly using the coherent interpretation of the key surfaces and comparing the systems tracts with the global sea-level curve, providing a more robust third-order sequential evolutionary model that includes three depositional sequences. The Middle Ordovician sheet braided deposits are the lowstand sediments of Sequence 1 truncated by an extensive unconformity that possibly removed the transgressive and highstand strata. This unconformity generated by glacial dynamics lasted approximately 25 Myr during the Late Ordovician to early Silurian. The second sequence started with the advance of ice sheets in marginal areas of the basin, causing the deposition of ablation diamicton during the lowstand. The postglacial transgression is marked by ice rafted debris from icebergs deposited onto organic matter-rich

mud in the shoreface-offshore zone. The maximum flooding during the middle to late Silurian was succeeded by the highstand phase marked by the progradation of deltaic deposits. Biological activity is marked by the presence of polychaetes that reworked the marine seafloor. The Early Devonian featured extensive sea-level fall and renewed continental drainage with the formation of a braided plain marking a lowstand phase of Sequence 3. These new interpretations allow the global correlation of the Serra Grande Group and provide an improved understanding of the role of ice sheets and postglacial transgressions that affected West Gondwana during the Ordovician-Silurian periods.

3.1 INTRODUCTION

The transition between the Ordovician and Silurian periods in the West Gondwana supercontinent was marked by a long glacial period, which climaxed during the Hirnantian (~445 Ma) (Ghienne 2003). The lower Paleozoic was characterized by climatic greenhouse conditions, with high CO₂ content in the atmosphere, five times greater than the current level (Brenchley *et al.* 1994, 2003). The migration of the supercontinent Gondwana towards the South Pole was concomitant with astronomical factors such as changes in the rotation of the Earth and a decrease in solar radiation that favored the growth of ice sheets (Brenchley *et al.* 1994). The end of the glaciation records the most considerable eustatic sea-level rise in Earth history, generating significant marine transgressions that started in the Llandovery (~443 Ma) and ended in the Ludlow (~423 Ma) (Haq & Schutter 2008). One of the best records of these events in West Gondwana is the Serra Grande Group (SGG), which represents an Ordovician-Devonian siliciclastic succession exposed in the eastern Parnaíba Basin, northeast Brazil. The group is subdivided into the Ipu (sandstones and conglomerates), Tianguá (shales and sandstones), and Jaicós (sandstones) formations. Most of the previous work on this group is strictly regional and lithostratigraphic, which has not allowed determining the depositional environments and systems based on a precise stratigraphic framework and has hindered the correlation with other Silurian successions of West Gondwana.

In this paper, we reinterpret the Ordovician-Devonian succession of the SGG cropping out in the region of Ipueiras, eastern Parnaíba Basin, northeastern Brazil, previously described by Barrera *et al.* (2018), Assis *et al.* (2019), Janikian *et al.* (2019) and Caputo & Santos (2019) (Fig. 1). Direct comparisons are made only with the work of Assis *et al.* (2019) because it is the only paper that presents a detailed stratigraphic framework. The depositional processes and environments from which these deposits were generated have been the subject of extensive discussions within the Brazilian scientific community. Based on sedimentological, stratigraphic, and facies analyses, we refine the previous sedimentary proposals for these deposits. These new interpretations allow us to improve the correlation of these deposits with other successions and to understand the role of ice sheets and postglacial transgressions that affected West Gondwana during the Silurian period.

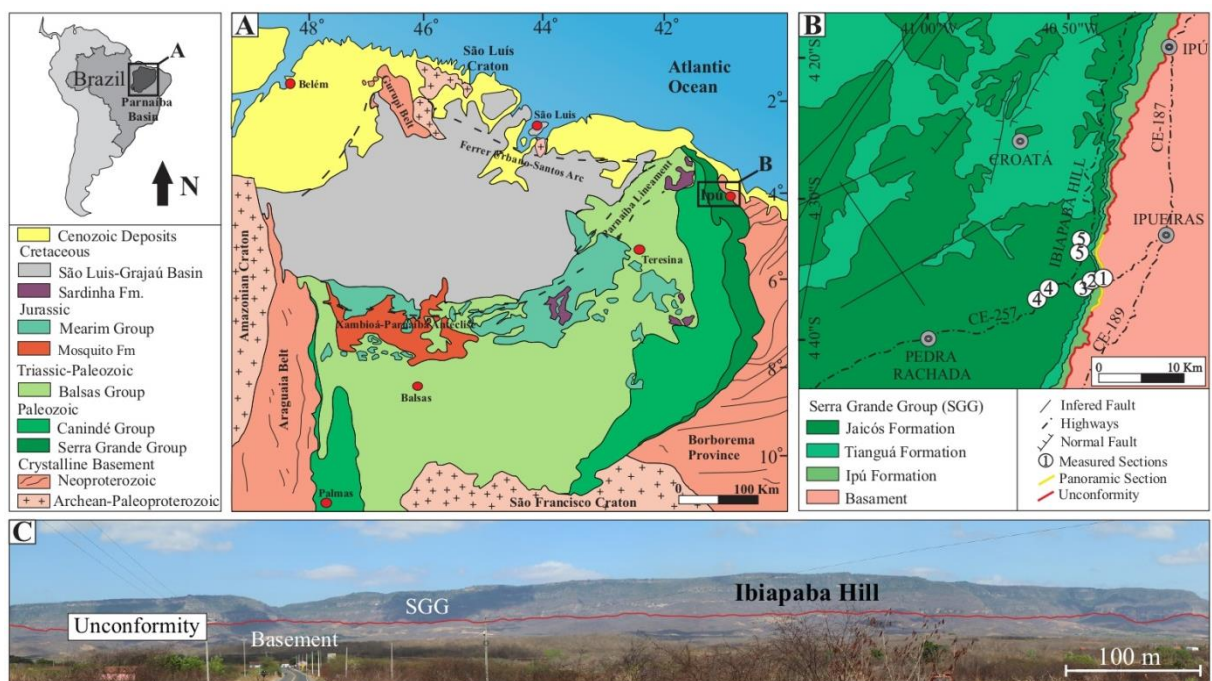


Figure 3.1- The Parnaíba Basin in northern Brazil and the study area location. A) Simplified geology of the basin. B) Geological map of the Ipueiras district region of Ibiapaba Hill with the locations of visited outcrops. C). Panoramic section of Ibiapaba Hill with indication of a regional unconformity (red line) at the base of the Serra Grande Group (SGG). Geological map at 1:100,000 of the Ipueiras district extracted from the database of the Geological Survey of Brazil (CPRM 2013).

3.2 GEOLOGICAL SETTING

3.2.1 The Parnaíba Basin

Classified as an intracratonic Paleozoic basin, the Parnaíba Basin is located in the northern part of the South American continent, northeastern Brazil, with an area of approximately 600,000 km², and its strata can reach 3.4 to 3.5 km thick in depocenters (Caputo 1984, Daly *et al.* 2014, Vaz *et al.* 2007). This basin, defined as the sag type (Daly *et al.* 2014), has low and localized subsidence rates controlled by orogenic cycles unrelated to tectonic plate boundaries (Daly *et al.* 2014). The origin and evolution of the Parnaíba Basin are mainly related to tectonomagmatic events (Daly *et al.* 2014), which produced the onset of sedimentation during the Paleozoic from an Ordovician depression caused by isostatic adjustments and cooling after the assembly of Gondwana (Brito Neves *et al.* 1984, Castro *et al.* 2014). The basin basement is mainly represented by igneous, metamorphic, and sedimentary rocks, with ages ranging from the Archean to the Ordovician, formed or reworked during the Brasiliano-Pan-African cycle (Vaz *et al.* 2007). During the early Paleozoic, an erosive surface developed on the basement (Fig. 1C), which represents the transition from the basement to the sedimentary infill of the Parnaíba Basin (Daly *et al.* 2014, Porto *et al.* 2018, Vaz *et al.* 2007). Góes & Feijó (1994) separated the stratigraphy of this basin into five sequences: Silurian Sequence (SGG); Devonian Sequence (Canindé Group); Carboniferous-Triassic Sequence (Balsas Group); Jurassic Sequence (Mearim Group) and Cretaceous Sequence (Grajaú, Codó, and Itapecuru Formations). The SGG deposited between the Ordovician to Early Devonian periods represents the first depositional supersequence recorded in the Parnaíba Basin (Vaz *et al.* 2007).

3.2.2 The Serra Grande Group

The Ipu Formation was discordantly deposited over the basin basement and exhibits a transitional contact with the Tianguá Formation (Caputo & Lima 1984). These deposits are mainly composed of sandstones, conglomerates, coarse sandstones, and diamictites, with thicknesses up to 300 m in the northeastern part of the basin (Caputo & Lima 1984). Kegel (1953) described some faceted pebbles within diamictites located in the upper portions of the Ipu Formation, which were later interpreted as glacial in origin. Caputo & Lima (1984) interpreted the basal and middle portions of the Ipu Formation as deposited within river systems that supplied the sediment for deltaic systems developed within marine environments in the western portion of the basin.

The Tianguá Formation has a maximum thickness of up to 270 meters in the subsurface and 150 meters measured in outcrops on the eastern edge of the basin (Caputo & Lima 1984). Rodrigues (1967) used the term Tianguá to identify a sedimentary succession composed of black shales, siltstones, and fine sandstones, described in outcrops within the region of Tianguá municipality in the northeastern basin. These sediments are interpreted as having been deposited within shallow marine and deltaic systems (Caputo & Lima 1984, Grahn & Caputo 1992, Grahn *et al.* 2005, Le Hérissé *et al.* 2001).

The Jaicós Formation was proposed by Plummer (1946) to designate a sedimentary succession present in the slopes of the Serra Grande in the northeastern part of the basin. This unit consists mainly of coarse sandstones, interpreted as having been deposited within river and delta environments, with maximum thicknesses of up to 400 meters in the subsurface and 200 meters at the surface (Caputo & Lima 1984, Vaz *et al.* 2007). The Jaicós Formation concurrently overlaps the Tianguá Formation, and its upper portion is limited by a regional unconformity that separates it from the Itaim Formation (Canindé Group) (Caputo & Lima 1984).

3.2.3 Age constraints

During recent decades, many works have had the main objective of establishing the stratigraphic position of the SGG. These studies were based mainly on paleontological interpretations, principally driven by the hydrocarbon industry (Caputo and Lima 1984, Grahn *et al.* 2005, Le Hérissé *et al.* 2001). For the Ipu Formation, Grahn *et al.* (2005) defined a middle Llandovery age, determined mainly by the presence of chitinozoans (*Cingulochitina bouniensi*; *Pogonochitina tianguaense* n. sp.; and *Sphaerochitina palestinaense* n. sp.). Analyses performed on Tianguá Formation rocks based on the identification of palynomorphs and graptolites (*Climacograptus* cf. *scalaris scalaris*) allowed us to define a middle Llandovery age for their basal portions (Grahn *et al.* 2005, Le Hérissé *et al.* 2001). The end of the Tianguá Formation deposition possibly coincided with the major transgressive events recorded globally during the Silurian (~423 Ma) (see Haq & Schutter 2008). Grahn *et al.* (2005), based on interpretations of chitinozoans (*Ramochitina* sp.), present in the upper portions of the Jaicós Formation, defined a Pragian age (Lower Devonian), for their final stages of deposition. Based on the data presented, it is essential to highlight that the best age defined within the SGG for its stratigraphic position is that of the Tianguá Formation.

3.3 METHODS

Five stratigraphic sections were measured in the eastern portion of the Parnaíba Basin, encompassing the Ipu and Ipueiras regions (Fig. 1B). Each sedimentary succession was logged bed by bed using outcrop-based facies analysis techniques (lithologies, sedimentary structures, paleocurrent data, and lateral and vertical variations), according to Walker (1992). The bed thicknesses were grouped as very thin-bedded (<1 cm); thin-bedded (1-10 cm); medium-bedded (10-30 cm); thick-bedded (30-100 cm); and very thick-bedded (>100 cm) (Ingram, 1954). Sequence stratigraphy techniques and concepts (Cateneanu 2019, Christie-blick *et al.* 1995, Kerans & Tinker 1997, Sarg 1988, Vail 1987, Van Wagoner *et al.* 1988, Zecchin *et al.* 2015) were experimentally applied to the SGG, and the individual analyses of outcrops were mainly focused on recognizing parasequences, key layers and discontinuity surfaces. The excellent exposures allowed the full mapping of all these surfaces and implied the possible genesis and stratigraphic significance of the discontinuity surfaces based on the facies associations and their positions within the studied succession. For a comprehensive sequence stratigraphic framework, the key surfaces, stacking patterns, systems tracts, sequences, and scales of observation were defined by high-resolution sequence stratigraphic techniques for siliciclastic deposits (Catuneanu 2019, Zecchin & Catuneanu 2013). Sedimentological cycles (i.e., beds and bedsets) are the building blocks of the lowest rank systems tracts and component depositional systems (Catuneanu 2019). In contrast, stratigraphic cycles (i.e., sequences) reflect changes in systems tracts and component depositional systems. Both types of sedimentary cycles involve changes in the stratal stacking patterns. Sedimentological stacking patterns refer to the stratal architecture that describes the internal organization of a depositional system without changes in the systems tract. In this work, an individual sedimentological cycle is approximately a parasequence.

The quantification and description of the primary and authigenic mineralogies of the sandstones were based on petrography of thin sections under an optical microscope (Galehouse 1971). To test for the presence of glaciotectonic microstructures in diamictite, such as alignment, crushing, and rotation of grains, microfaults and microfolds were used, as in the works of Van der Meer (1993), Menzies *et al.* (2016) and Bustfield & Le Heron (2016).

3.4 FACIES ANALYSIS

The fieldwork carried out on outcrops located in a continuous succession of the SGG presents roadcut sections along the CE-257 highway crossing Ibiapaba Hill (Fig. 1). Seventeen sedimentary facies are described in an ~170 m-thick succession of the SGG and grouped into seven facies associations (FAs), which represent the evolution of preglacial (FA1), glacial (FA2, FA3, and FA4) and postglacial (FA5, FA6, and FA7) deposits (Fig. 2). The fresh color is gray to dark, while weathered facies have reddish and sometimes whitish to yellowish coloration.

3.4.1 Tabular cross-bedded conglomerate and sandstone facies association (FA1)

Description

FA1 is 47 m thick and presents lateral continuity of up to 300 meters (Fig. 2). The deposits of FA1 consist of stacks of laterally continuous tabular bodies, with thicknesses ranging from 40 cm to 80 cm. The deposits show indistinct or incipient fining-upward cycles composed of a mixture of sandstone and conglomerate beds that sometimes pinch out laterally (Fig. 3A). The contacts between the facies are mainly flat, and subordinate erosive contacts have been identified in the middle portion of the association. Medium- to coarse-grained sandstone and conglomerate exhibit cross-bedding to low-angle stratification and even parallel stratification. Subordinate levels of massive conglomerates change laterally to pebbly sandstone occurring preferentially at the bases of cycles (Fig. 3B). The lithofacies are moderately well sorted and texturally mature. The rock framework exhibits angular to subangular grains with low sphericity. The grains are predominantly quartz and metamorphic and sedimentary rock fragments and secondarily feldspars and heavy minerals. Imbricated clasts are commonly observed, and coarse grains are segregated in the foresets and at the base of sets forming lags (Figs. 3C and D). The cross-strata show preferential migration towards the NW.

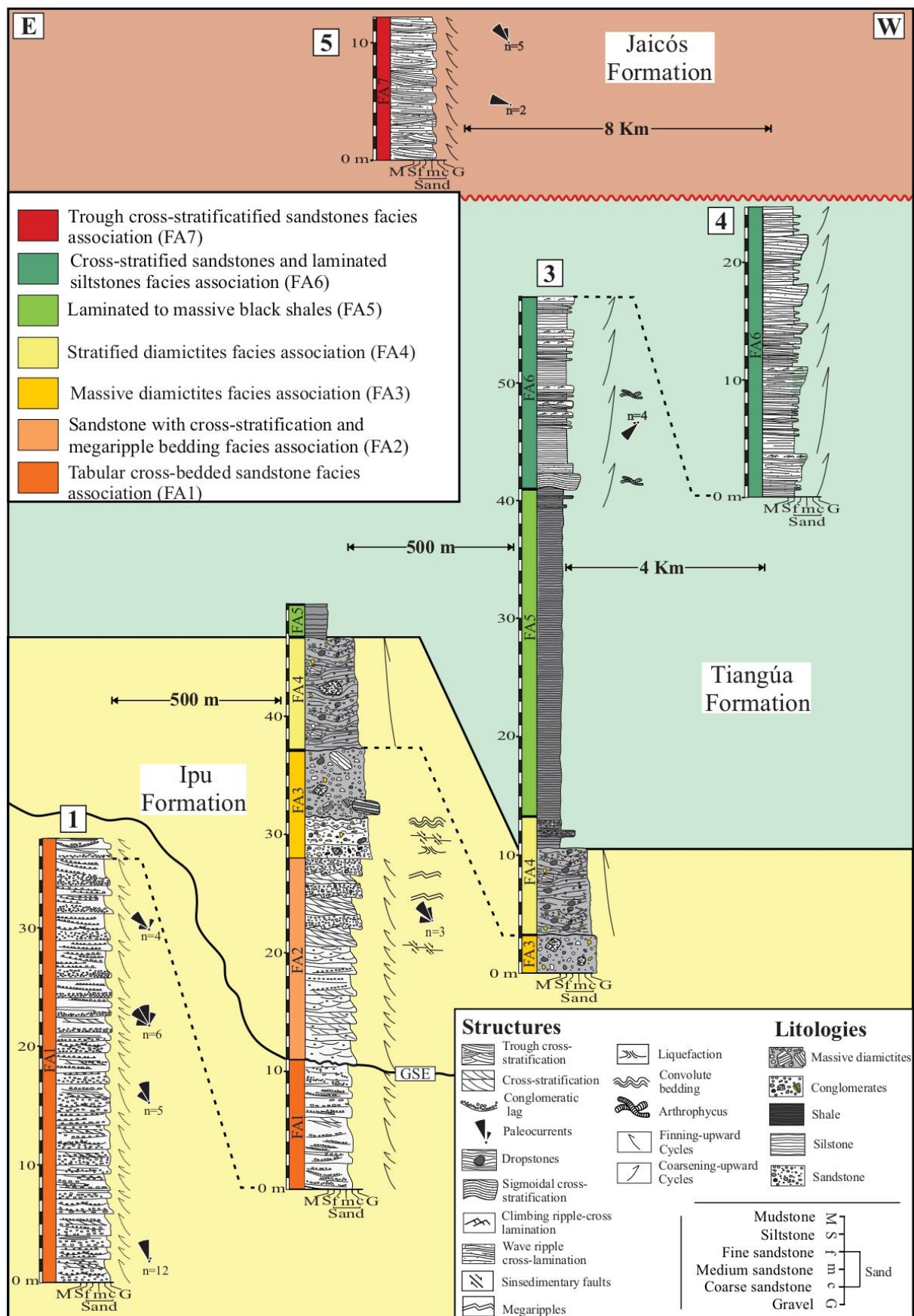


Figure 2. Sedimentary logs and descriptions of facies associations in the Serra Grande Group in the Ipueiras region, eastern Parnaíba Basin, northeastern Brazil. Note the glacial surface erosion (GSE) on the basis of FA2.

Interpretation

The predominance of tabular beds up to 80 cm thick and laterally continuous for hundreds of meters suggests sand deposition from unconfined flows on planar surfaces, indicating widespread deposition in shallow and broad channels or plains. The high width/thickness ratio of the channel is compatible with a shallow and laterally continuous morphology (see Long 1978). The presence of even parallel stratification and low-angle foresets suggests high-energy and sheet flow conditions. The thinness of incipient cycles indicates little generation of accommodation space or shallower conditions as a response to channel margin instability with continuous reduction of water laminae (Schumm 1968). The change from a high to a lower flow regime is evidenced by the variations in sedimentary structures upward within the cycles, from even parallel to low-angle stratification to cross-bedding. Fine sediments and small-scale sedimentary structures are not observed at the top of cycles, indicating low preservation or extreme fluvial erosion, which confirms the high-energy conditions within a bedload river system (Long 1978). The kind of river is characterized by a wide lateral distribution of the bodies, suggesting the instability of the river bars and margins (Davies *et al.* 2011, Schumm 1968). The variables mentioned above configure a specific morphology defined as pre-vegetational sheet braided river channels (Cotter 1977, Hjellbakk 1997). Vegetation is a controlling factor of channel morphology (Miall 1981) with implications for the geometry of the bedforms. Sediments without vegetation are 20.000 times less stable than those with 16% to 18% root plants (Smith 1976). The absence of thick flood deposits, a characteristic of braided rivers, increases the migratory tendency of channels. The fluvial channels are predominantly straight, with little variation in the direction of the paleocurrents (Long 1978). These distributaries allowed the migration of sand flats and 2D and 3D dunes, as well as the displacement of gravel sediments under a lower flow regime (Ielpi & Rainbird 2015).

The fluvial facies rarely present a well-defined cycle array. The homogeneous granulometry and the occurrence of one or two types of principal structures, predominately tabular to low-angle cross-bedding, hinders the identification of cyclicity and is typical of the pre-Silurian fluvial system. The predominance of coarse-grained sandstones and conglomerates with clasts that reach up to 3 cm and eventually cobbles and boulders indicate an intermediary braided plain distant from the source area.

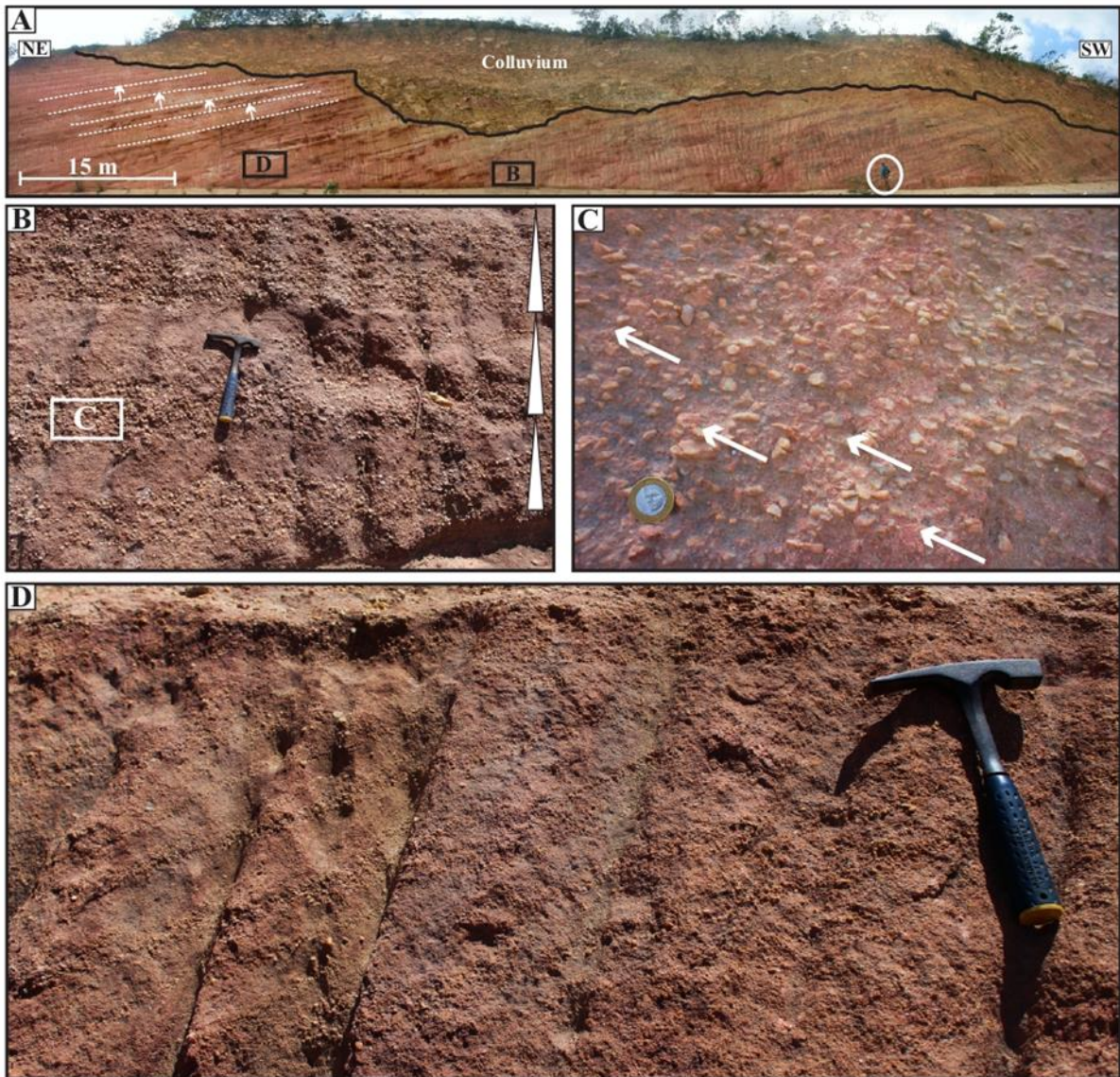


Figure 3. Faciological aspects of FA1. A) Panoramic section depicting the fining-upward cycles (arrows) in the tabular sandstones with cross-bedding. Note a 1.85 m-tall geologist for scale inside the white circle. B) Detail of the incipient fining-upward pattern in FA1, represented by white triangles. C). Imbricated clasts observed in the bottom of an incipient fining-upward cycle. D) Cross-stratified sandstone facies with coarse particle size segregation in the foresets.

3.4.2 Sandstone with cross-stratification and megaripple bedding facies association (FA2)

Description

This association is up to 17 m thick and laterally continuous for approximately 250 meters (Fig. 2). FA2 consists of medium- to coarse-grained sandstones with cross-stratification and some megaripple bedding (Figs. 4A, B, and C). The rock framework is texturally mature with moderately sorted, subangular to subrounded grains with medium sphericity. Pebbles and cobbles and locally boulders of quartz and metamorphic, sedimentary, and igneous rocks predominate (Fig. 4). These facies exhibit sets of small- to medium-scale

trough stratification to low-angle cross-stratification that are 30 cm to 80 cm thick and laterally continuous up to 30 m (Fig. 4C). Isolated pebbles are observed following the foreset dips (Figs. 4D and E). Locally, clast-supported conglomerates form lenticular bodies with massive bedding and even parallel to low-angle cross-stratification, apparently composing the bases of centimeter-scale fining-upward cycles (Fig. 4A, B and C). The conglomerate often abruptly overlies cross-stratified pebbly sandstone with flat and sharp contacts, sometimes with load cast features (Figs. 4D and E). Deformed structures are found mainly in siltstone and sandstone beds and consist of microfaults and convolute bedding (Figs. 5B to E). Paleocurrent measurements in cross-stratified sandstone indicate preferential migration towards the NW.

Interpretation

The intercalations between massive to stratified clast-supported conglomerate and cross-bedded sandstone record fast deposition and high energy with variations between the upper and lower flow regimes. Gravel was deposited under hyperconcentrated flows, contrasting with the low-concentration flows responsible for sand deposition in a subaqueous setting (e.g., Hornung *et al.* 2007, Le Heron *et al.* 2012, Russell & Arnott 2003). The sharp limits of the beds suggest a faster change in flow than the transitional energy level. These variations are attributed to the continuous alternation of sedimentary charges directly linked to the increases and decreases in meltwater discharge (see Hornung *et al.* 2007). In general, the overall upward increase in the sediment grain-size pattern (FA2 to FA3) represents a gradual approximation of the ice-sheet margin (Ghienne *et al.* 2007). In this environment, the laminar flow was episodically disturbed by ice rafted debris dumped on the substrate and afterward reworked and redeposited. The pebble clasts present on the sandstone cross-strata correspond either to isolated clasts that act as remains when finer material has been removed by ice-melting water or to dropstones (Ravier *et al.* 2014). Additionally, pebbles are incorporated in the foresets of migrating dune bedforms (Church & Gilbert 1975, McDonald & Vincent 1972, Russell & Arnott 2003).

The formation of dunes was conditioned by sustained flow and the continuous entry of sediments, which implies the presence of almost stable concentrated density flows (Ravier *et al.* 2014, Winsemann *et al.* 2007). Despite the laminar flow and alternation of the flow regime, the preservation of megaripple morphology indicates that suspension was a frequent process during the migration of bedforms. Due to the predominance of redeposited sediment, it is more likely that the depositional environment of FA2 was not in direct contact with ice

sheets. The possibility of these deposits being supplied by subglacial conduits through a series of submarine jet effluxes in ice-sheet marginal settings over a distance of several hundred meters or kilometers has not been discarded (e.g., Hornung *et al.* 2007, Le Heron *et al.* 2012, Russell & Arnott 2003). The jet efflux framework is defined as the distal zone of established flow, characterized by the presence of tractional bedforms combined with fluctuating suspension fallout (Hornung *et al.* 2007, Russell & Arnott 2003). After deposition, the water oversaturated sediment was subjected to liquefaction processes that generated a series of soft-sediment deformation features modifying the primary framework (Cheel & Rust 1986).

3.4.3 Massive Diamictites facies association (FA3)

Description

FA3 is 12 m thick, forms tabular beds laterally continuous for hundreds of meters and consists of two types of matrix-supported conglomerate/diamictite generally cemented by silica and clay minerals (Figs. 2 and 6). Polymictic, matrix-supported diamictites exhibit rounded to subangular clasts of different compositions (gneiss, granite, basic volcanic rock, quartzite, schist, sandstone, pelite, quartz) ranging in size from granules to boulders, often faceted and striated. Sandy-clayey matrix-supported diamictite is less common in FA3 and forms thin massive beds, eventually alternating with clay matrix-supported diamictite forming beds up to 3 m thick (Fig. 5). The clasts reach cobble size, with compositions mainly of quartz and metamorphic, igneous, and sedimentary rocks that are entirely scattered in the chaotic rock framework (Fig. 5A). The diamictites are poorly sorted and texturally immature and contain angular grains with low sphericity (Figs. 6A, B and C). The quartz grains present conchoidally fractured, striated, crushed, and smoothed surfaces (Figs. 6D and E). Striated, faceted, and disseminated clasts frequently deform the basal laminae (dropstones and bullet-shaped clasts). Convolute bedding occurs sporadically.

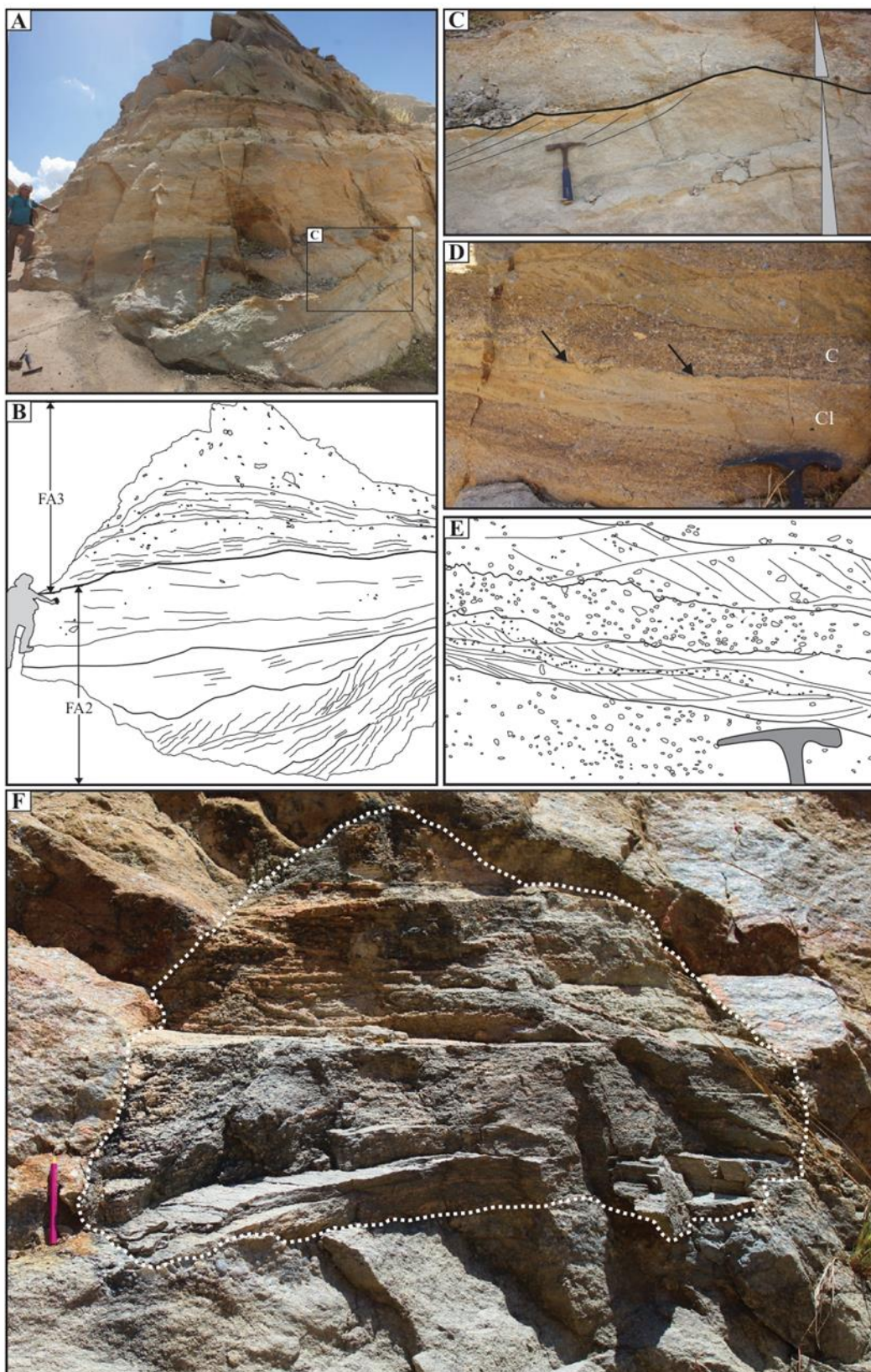


Figure 4 Faciological aspects of FA2. A) and B) Contact between massive diamictite (FA3) and conglomerate interbedded with sandstone exhibiting normal gradation, megaripple and low-angle cross-bedding. C) Detail of A) showing megaripple bedding with well-defined limits, graded beds and cross-bedding. D) and E) Cross-laminated fine sandstone (Cl) alternating with even parallel stratified conglomerate (C); note the granulometric segregation in the foresets with clasts following the cross-strata and load casts (arrows). F) Megaclast of banded gneiss (the scale is a pencil of 15 cm).

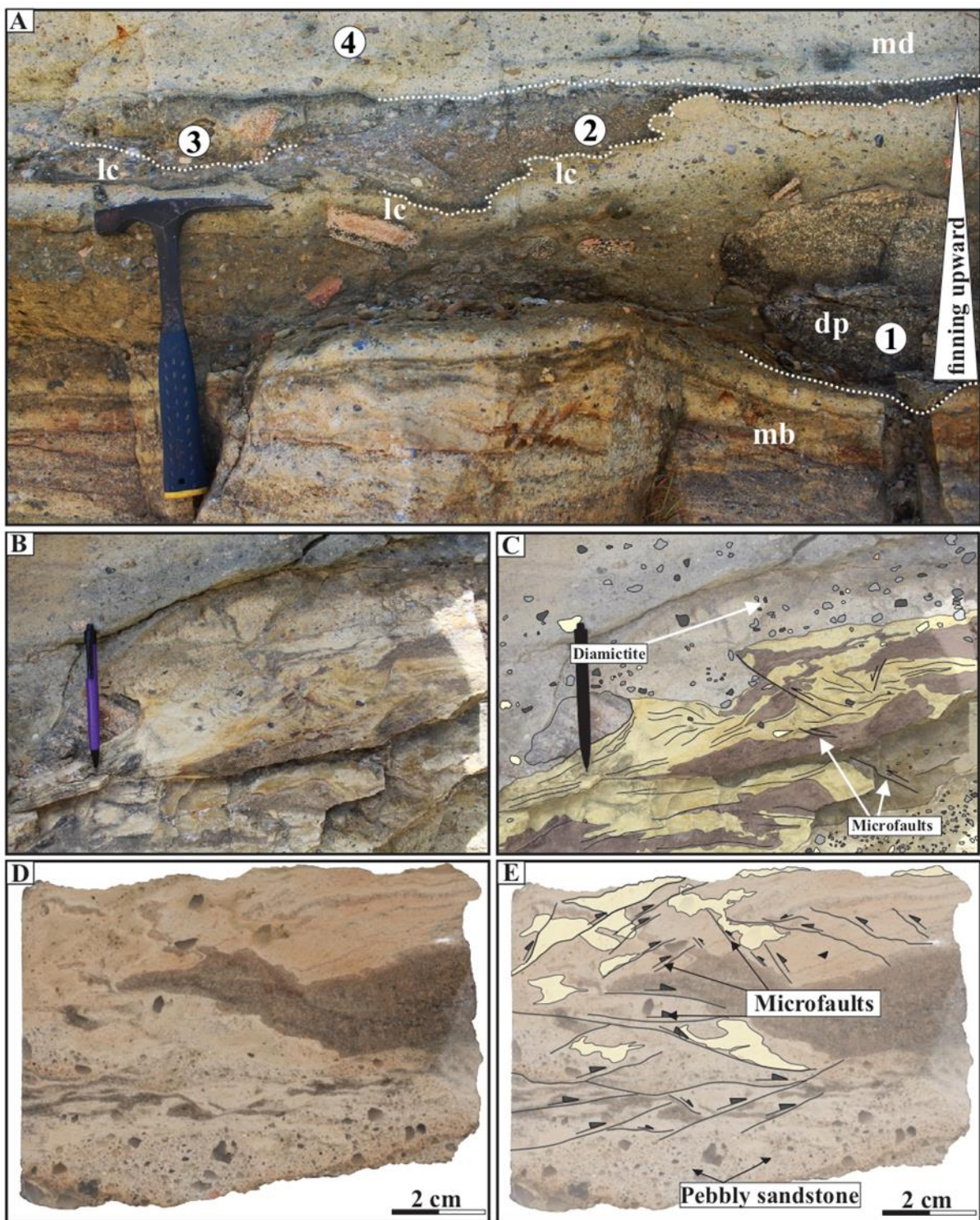


Figure 5. Deformational features in the contact zone between FA2 and FA3. A) Megarippled bedded sandstone (mb) underlain by distinct intervals of diamictite (1-4) with dropstone (dp) and load cast (lc) features. Note in A) the fining-upward cycle (1) overlying megarippled bedded sandstone and underlain by massive diamictite intervals. F) and G) Contact between massive diamictite of FA3 overlying siltstone and sandstone of FA2 with convolute bedding and microfaults. E) and F) Details of the contact between massive pebbly sandstone and conglomerate with microfault and convolute bedding.

Interpretation

This facies association is interpreted as subaqueous glaciogenic deposits of cohesive debris flows deposited from the ablating ice front or as flow tills (Hornung *et al.* 2007, Le Heron *et al.* 2012, Lønne 1995). Massive diamictites are texturally comparable with ‘plug flows,’ which are deposits released from meltwater point sources on an ice-contact fan (Powell 1990). Similarly to the FA2 conglomerate, these deposits were generated by jet efflux inside the zone of flow establishment (Hornung *et al.* 2007). In this region in front of the ice sheet, the deposition is characterized by hyperconcentrated density underflow sediments generated by the fallout of coarse sediment from turbulent suspension (Hornung *et al.* 2007, Russell & Arnott 2003). This process explains the lack of internal structures in the beds (Le Heron *et al.* 2012). The excess pore water pressure in the sediment increased the load, compatible with deposition in the subaqueous fan (Cheel & Rust 1986). The lack of vertical variations in the granulometry of diamictites suggests that the ice sheets were probably stationary, producing an aggradational accumulation of poorly immature sediment in moderately deep waters devoid of strong currents. This hydrodynamic behavior suggests that the grounding line was quasi-stable during deposition over time (Powell 1990). The microtextures observed on the grain surfaces corroborate transport and deposition influenced by glacial processes (see Ó Cofaigh *et al.* 2005, Tulaczyk *et al.* 1998).

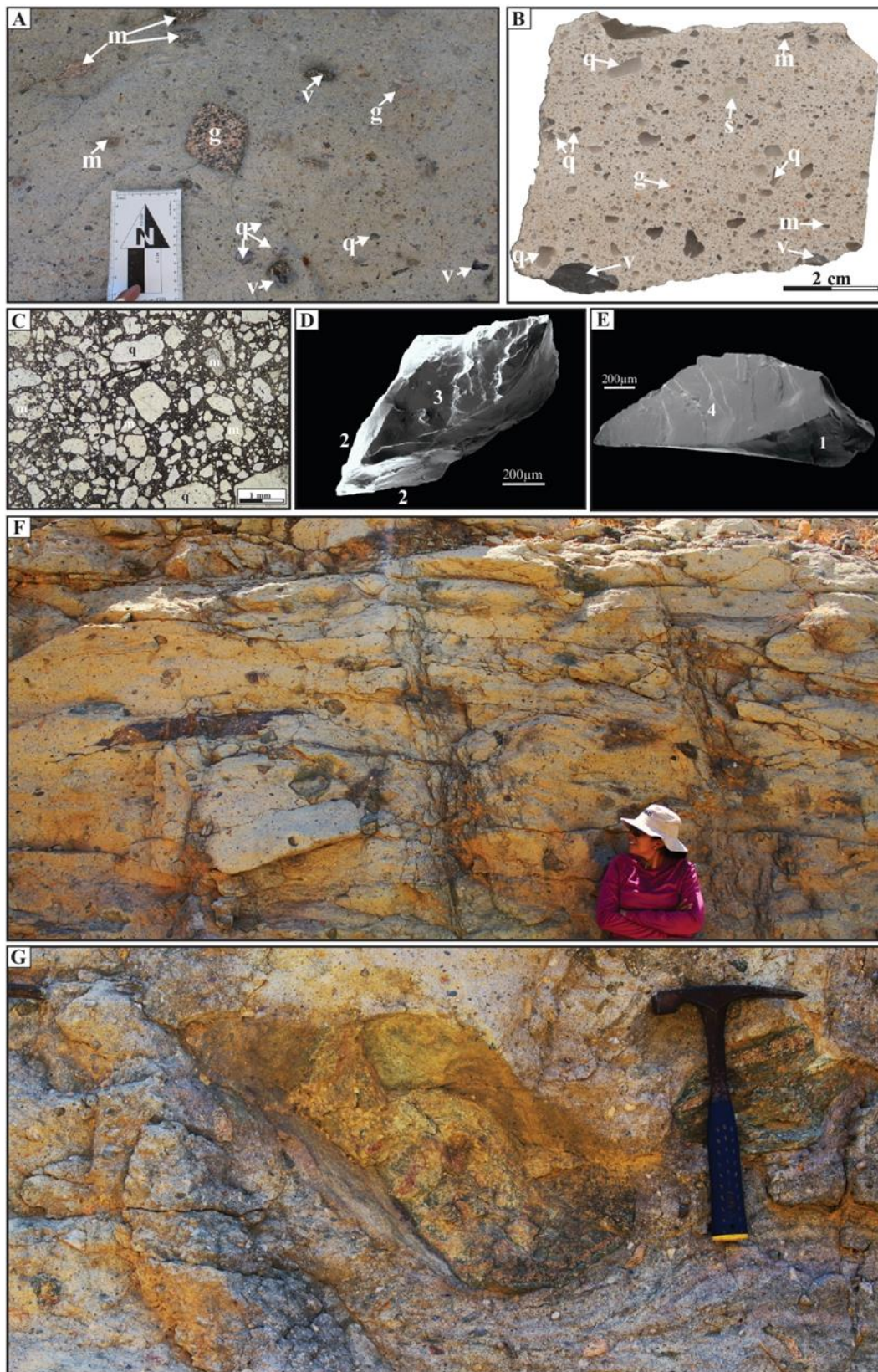


Figure 6. Textural and faciological aspects of FA3 (A to E) and FA4 (F-G). A) and B) Massive diamictite with angular to subrounded clasts of wide compositional variety (m-metamorphic, q-quartz, v-volcanic, g-granite, s-sedimentary). C) Petrographic aspect of massive diamictite. D) and E) Scanning electron microscopy (SEM) images showing microtextures observed on quartz sand grain surfaces that include conchoidal fracture (1), striated surface (2), crushing surface (3), and smoothed surface (4). F) Stratified diamictite. G) Dropstones deforming basal strata in diamictite.

3.4.4 Stratified diamictites facies association (FA4)

Description

FA4 is 11 m thick and laterally continuous for hundreds of meters and is composed of stratified diamictites and black shales with drop clasts ranging from a few centimeters to 70 cm in diameter (Figs. 2, 6G and 7A to C). The stratified diamictites consist of tabular beds and lenses between 0.3 and 1.2 m thick with incipient or even parallel stratification (Fig. 6F). Compositionally, the fragments are quartz and metamorphic, igneous, and sedimentary rocks that float within a sandy to silty matrix. These lithofacies are poorly sorted and texturally immature. The grains that constitute the framework exhibit mostly angular to subangular morphologies and low sphericity. The clasts display a faint orientation following even parallel stratification (Fig. 6F). Metric limestones occur at the base of FA4, while pebbles with similar compositions in stratified diamictite predominate towards the top. The organic matter-rich black shale consists of centimetric beds that alternate with quartz drop clasts and isolated lenses of massive diamictite (Figs. 7B and C).

Interpretation

FA4 is interpreted as sediment deposited within a proglacial environment (glaciomarine), implied by the negative variation in the mass balance of ice sheets, from which large amounts of water and debris were released feeding this marine system (Lønne 1995, Miller 1996, Visser 1997). The stratified diamictites represent deposits generated by debris flows with higher inputs of silt and clay that settled during ice margin retreat (Visser 1997). Stratification was generated during high meltwater outflow rates and sediment gravity flows (Visser 1997). The viscosity of debris with low water content was influenced by weak currents causing poor sediment segregation and generating incipient stratification and clast imbrication. Clay and silt with high organic matter contents were deposited by suspension settling from sediment-laden meltwater plumes in a glacially influenced marine environment (Visser 1991). The initial phase of postglacial transgression was influenced by ice-shedding and iceberg calving processes, or rainout from the ice shelf produced a variety of structures characteristic of underwater systems such as dropstones and dumpstones (Boulton 1981, Eyles 1993, Hart & Roberts 1994, Miller 1996, Zecchin *et al.* 2015). A fining-upward pattern in a glaciogenic succession typically indicates a density decrease associated with depositional processes since ice rafted debris to suspension load suggests that deposition was occurring

progressively farther from the glacier margin following the glacial retreat (Boulton, 1981). The black shales with debrites were probably deposited in the offshore zone.

3.4.5 Laminated to massive black shales facies association (FA5)

Description

This facies association comprises thick black shale packages composed of the intercalation of centimetric massive and laminated argillaceous beds rich in organic matter (Fig. 7A). The contacts between the facies are mainly flat. FA5 deposits have thicknesses of up to 30 meters and lateral continuity of up to hundreds of meters (Fig. 2). Unlike argillaceous deposits in the stratified diamictite facies association, this facies association does not include structures generated by ice-raftered debris processes.

Interpretation

The maximum flooding after postglacial transgression increased the accommodation space, enlarging the marine platform. The deposition of the black shales was the result of suspension settling of clay and silt in deep waters influenced by progressive sea-level rise linked to a long-term transgression. The black shales were deposited in deep waters related to a low-energy depositional setting, probably in the offshore zone (Reading & Collinson 1996). Structures related to storm and oscillatory flows are not observed in this facies association and confirm this interpretation.

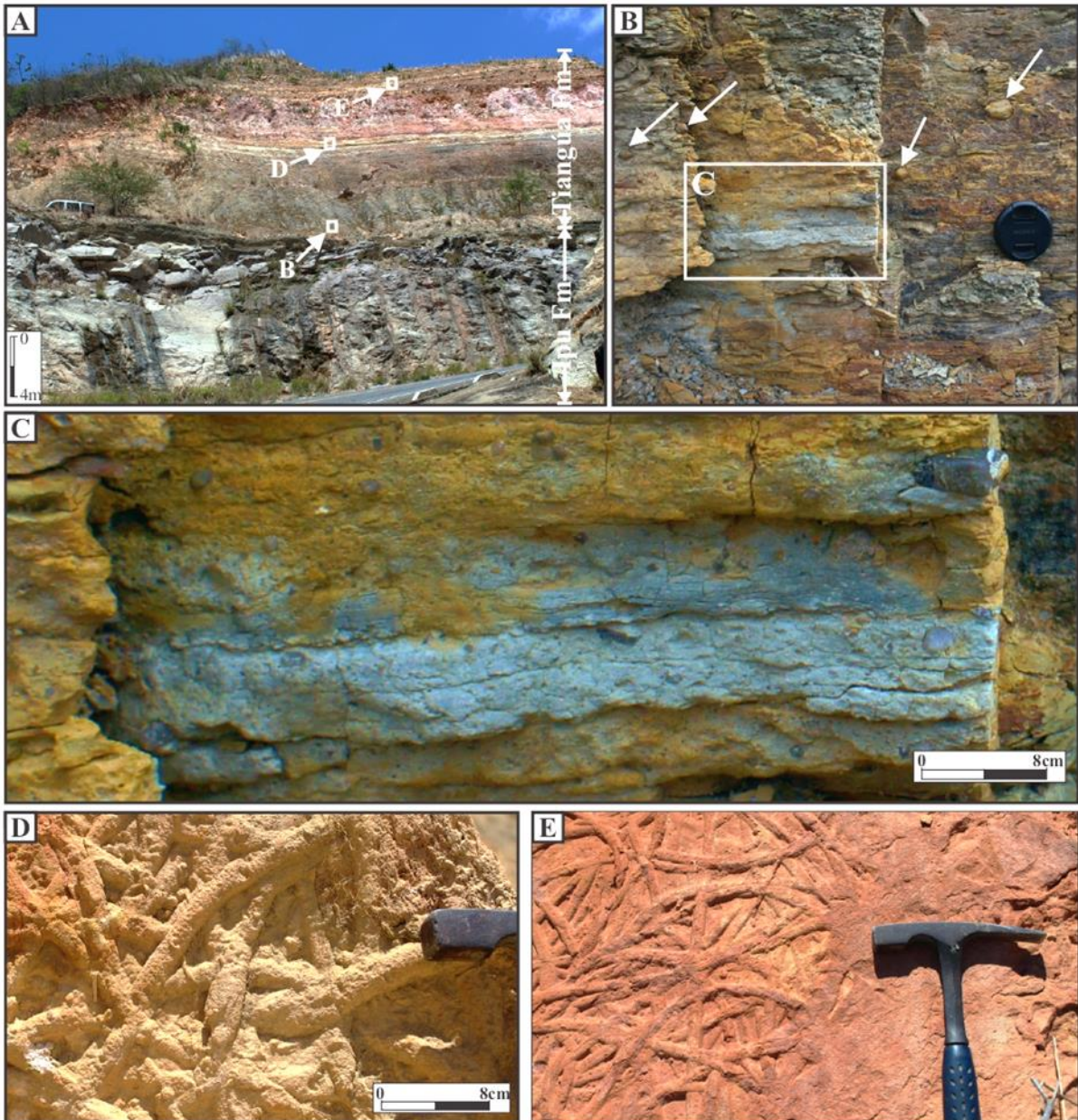


Figure 7. Faciological aspects of FA4, FA5 and FA6. A) Contact between the laminated to massive black shale facies association (FA5) and the cross-stratified sandstones and laminated siltstone facies association (FA6). B) Detail of A), exhibiting dropstone (arrows) and dumpstone (rectangle) structures present in FA4. C) Detail of B), showing the composition of the diamictites that compose the dumpstone structures. D) and E) Details of two different types of ichnotaxon *Arthropophycus* identified on FA6.

3.4.6 Cross-stratified sandstones and laminated siltstones facies association (FA6)

Description

FA6 is 40 m thick and forms tabular and lenticular beds of fine- to medium-grained sandstone and siltstone with lateral continuity for hundreds of meters (Figs. 8A and B). A sigmoidal lobe is the predominant geometry with a maximum thickness of up to six meters at the outcrop scale (Fig. 8). The rounded grains of quartz and feldspar are well sorted and have high sphericity. Sigmoidal to low-angle cross-bedding forms thicker beds interbedded with

centimetric layers with low-angle to even parallel lamination and subcritical climbing-ripple cross-lamination (Figs. 8C and D). These beds are organized in meter-scale coarsening-upward cycles, and the contacts between the facies are mainly flat (Figs. 8A and B). The sigmoidal lobes preferentially migrate to the SW (Fig. 2). Convolute beds and down-warped laminations deforming low-angle cross-stratification are consistent with water-escape structures, according to Frey *et al.* (2009) (Figs. 8E and F).

Hypchnial trace fossils of *Arthrophycus* are observed at the bases of coarsening-upward cycles associated with cross-laminated sandstone. These traces are horizontal to subhorizontal in a longitudinal section, found as tubes with positive hyporelief, concordant to subconcordant to the bedding and filled with fine-grained sandstone. The lengths of the analyzed specimens vary from 10 to 20 cm and from 1.5 to 3 cm in diameter in cross-section (Figs. 7D and E). Excavations usually have straight, branched, and curved shapes. Tunnel intersections are frequent and generally form angles from 90° to 100° (Figs. 7D and E).

Interpretation

Sigmoidal cross-bedding was formed during flow deceleration as a result of the entry of homopycnal flows into a marine system and the subsequent progradation of delta lobes (Mutti *et al.* 2003, Olariu *et al.* 2010, Reading & Collinson 1996, RØe 1987). The toe sets of sigmoidal lobes are dominated by suspension deposits and alternate with the migration of current ripples generating a rhythmite. The progradation of sand lobes over the toe sets produces the coarsening-upward pattern characteristic of deltaic successions (Bhattacharya 2006). The high rates of sand fallout and water-saturated sediments result in total or partial liquefaction and fluidization, which produce massive bedding and water-escape structures, respectively (Lowe 1975, Owen 2003). The weight of sandy lobes during rapid and successive progradation contributes to the soft deformation and loading of beds. The predominance of strata composed of medium-grained sandstone and low mudrock content indicates proximity to the coastline interpreted as a delta front (Galloway 1975). This association overlies the offshore deposits of FA5, indicating a diachronic association and a prodeltaic setting (Bhattacharya 2006). The occurrence of ichnotaxon *Arthrophycus* that resembles temporary feeding structure (fodinichinia) traces represents the proliferation of polychaetes in marine settings (Häntzschel 1975).

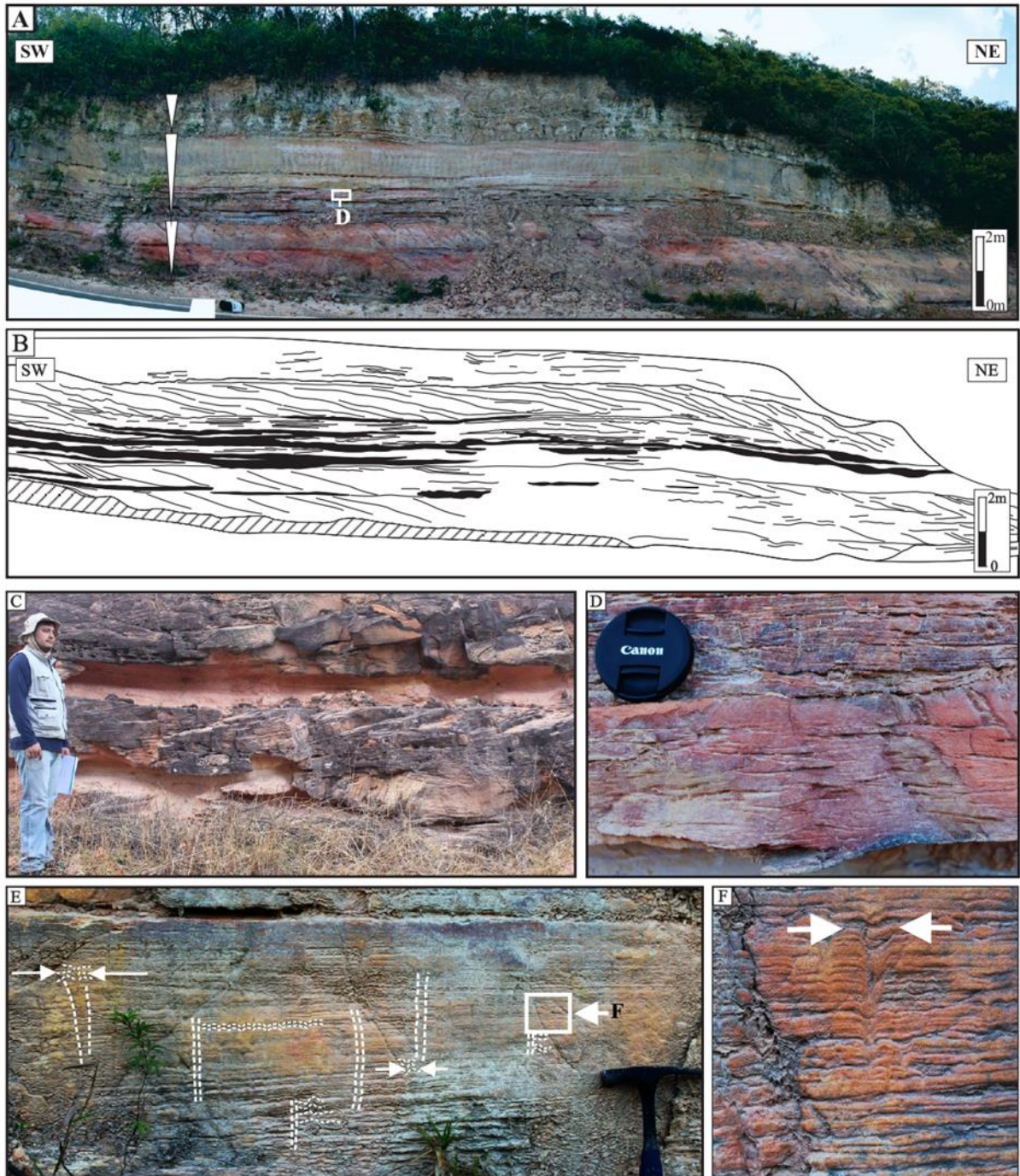


Figure 8. Faciological aspects of cross-stratified sandstones and laminated siltstones facies association (FA6). A), B) and C) Panoramic sections showing coarsening-upward cycles with lobe geometry formed by sigmoidal cross-strata and laminated siltstone interbedded with cross-laminated sandstone. D) Detail of A with subcritical climbing-ripple cross-lamination. E) and F) General view and close-up of water-escape structures identified in laminated fine-grained sandstone; note the down-warped laminations deforming low-angle cross-stratification.

3.4.7 Trough cross-stratified sandstones facies association (FA7)

Description

FA7 is 15 m thick and laterally continuous for hundreds of meters (Figs. 2 and 9). The deposits consist of stacked lenticular beds ranging from 0.80 to 1.2 m thick and composed of medium- to coarse-grained sandstones with trough cross-stratification and even parallel stratification (Figs. 9A, B and C). Cross-strata preferentially migrate to the NW (Fig. 9D). The sandstone is well sorted and texturally mature and composed mainly of rounded to subangular quartz grains with high sphericity. The succession is organized in fining-upward cycles whose semi-concave upward basal surfaces are underlaid by cross-stratified coarse sandstone that becomes more fine-grained to the top (Fig. 9A and B). The contacts between the facies are mainly flat to undulating, and subordinate erosional surfaces are common.

Interpretation

The facies assemblage of FA7 represents deposits related to high-energy flow linked to successive deposition by bedload currents with the migration of 3D bedforms (Ielpi & Rainbird 2015). In contrast to FA1, the dominance of lenticular beds suggests recurrent erosion of the substrate in shallow channels with low sinuosity with predominant unidirectional flow compatible with braided river systems (Gibling *et al.* 2014, Long 1978). The variables mentioned above configure a specific morphology defined as channeled braided (Cotter 1977).

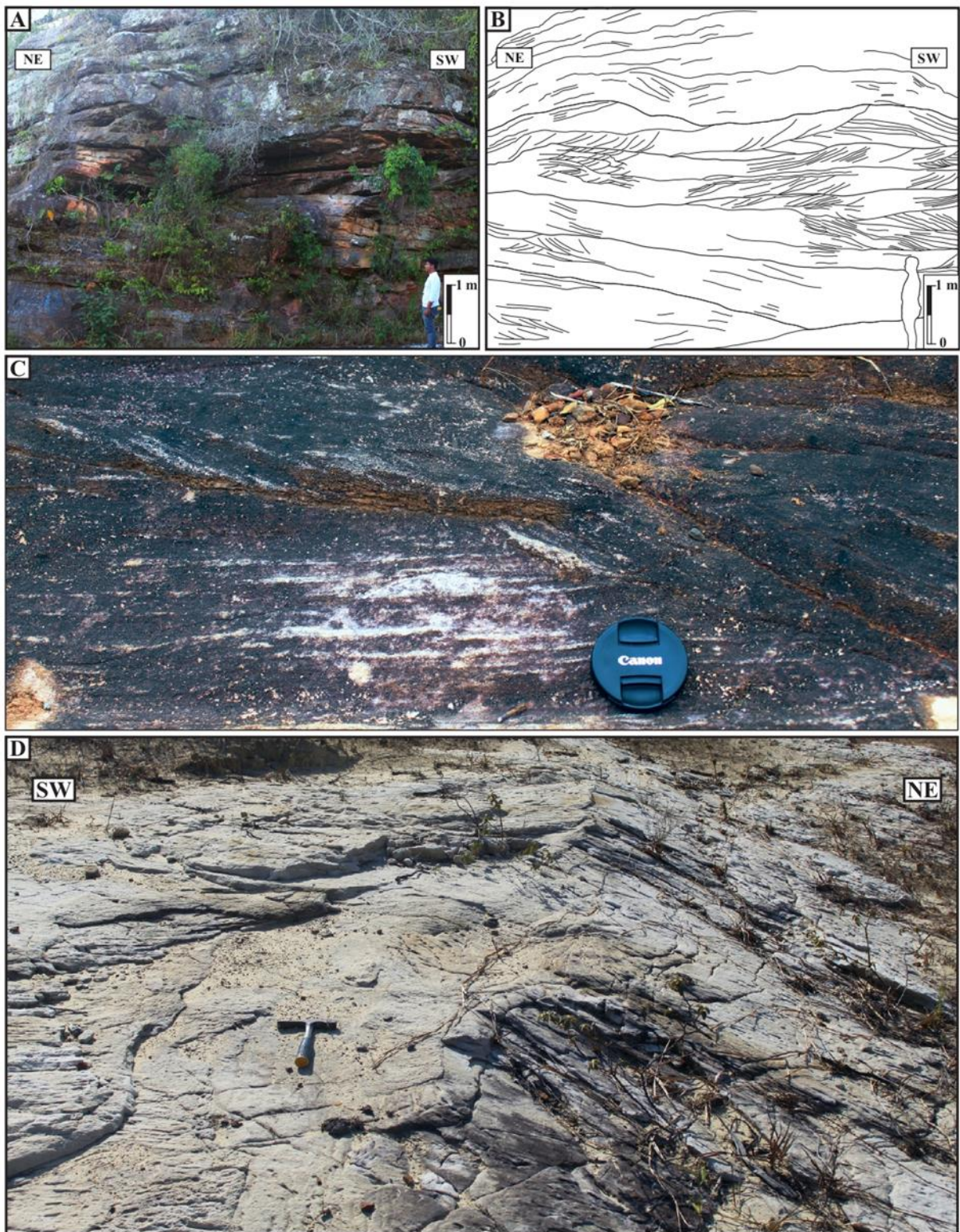


Figure 9. Faciological aspects of FA7. A) Lenticular geometry. B) Trough cross-stratification. C) Plane view of trough cross-stratification dipping to the NW.

3.5 FACIES MODEL

The outcrop-based facies and stratigraphic analysis of the SGG carried out mainly on the siliciclastic succession exposed in Ibiapaba Hill provides seven facies associations that exhibit continuous lateral distribution for hundreds of kilometers. The facies model for this group is developed using previous data, and new interpretations allow the correlation of depositional systems for other regions of the Parnaíba Basin. The facies model reveals a spatial and temporal evolution that includes fluvial (lower Ipu and Jaicós Formations) and glaciomarine to deltaic (upper Ipu and Tianguá Formations) settings. The record of the Silurian glaciation is composed of a single glacial cycle, consisting of deposits generated within ice-contact fans (FA2 and FA3) and proglacial environments (FA4 and FA5) (Fig. 10). Previous works have interpreted the glacial depositional system using only the occurrence of diamictites and striated clasts and pavements recognized mainly in drill cores and secondarily in outcrops (see Caputo & Santos 2019, Grahn & Caputo 1992). Glacial strata (mainly diamictites) interbedded with nonglacial strata might have influenced these authors in recognizing different glacial cycles in the lower Paleozoic succession of the Parnaíba Basin. The glacial deposits do not reach 20 m at the top of the Ipu Formation and represent a single glacial episode that affected the South American shelf during the early Silurian.

Tabular sandstones with cross-bedding in FA1 represent the installation of an extensive fluvial system (big river?), located directly on the basement. Assis *et al.* (2019) record putative alluvial fan deposits under basement rocks in the Ipu succession (Figs. 5 and 6. Pages 9 and 10). However, the outcrops described by these authors do not have physical continuity with the Ipueiras section and are difficult to include in the Ipu succession. Additionally, the interpretation of a fluvial system in the intermediary portion of the braided plain distant from the source corroborates the lack of preservation of alluvial fan deposits. Deposits related to this sizeable ancient river have been recognized throughout the east side of the Parnaíba Basin (Caputo & Lima 1984, Metelo 1999). Sandstones and conglomerates with thicknesses of hundreds of meters are interpreted as perennial pre-vegetational rivers probably fed by mountainous regions in West Gondwana before the Ordovician-Silurian glacial age. The interpretation of FA1 as a sheet braided river corroborates the previous interpretation by Janikian *et al.* (2019).

The glaciogenic sediments (FA2, FA3, and FA4) deposited during the glacial advance were continuously reworked by meltwater released from ice sheets. The sediments were transported by currents, debris flows, and ice-rafting processes in a subaqueous environment in the shoreface zone of a marine platform (Fig. 10). Megarippled bedded sands (FA2)

alternating with massive diamictons by ablation (FA3) represent ice-contact fan deposits (Fig. 10A). Textural differences in these deposits were controlled by the position of the jet efflux conduit and the influence of its hydraulic conditions on the distribution of sediments for shallow to deep waters (e.g., Hornung *et al.* 2007, Powell 1990). The quartz grain microtextures found in massive diamictite are analogous to those of flow-tilt deposits generated during ice sheet advance until the still-stand phase (Lønne 1995) (Fig. 10A). Stratified diamictons (FA4) were generated by ice rafted debris and tractive currents associated with the rapid release of abundant ice meltwater during the ice retreat phase (Fig. 10B). Debrites are found as dump features in the black shales, indicating the presence of icebergs in an ice-free sea. The fast velocity of ice meltwaters does not allow the development of 2D and 3D bedforms, forming only sand sheets during progressive retreat. Outwash plains and soft lodgment tills with striated pavements were inferred in the studied succession by Assis *et al.* (2019). Outwash plains are typically braided channels supplied by meltwaters in front of or beneath glacier ice (Boulton & Deynoux 1981, Ghienne 2003). The predominance of massively bedded diamictite, sporadic cross-stratified sandstone, and incipient fining-upward cycles suggests that much more ablation alternated with re-sedimentation processes by tractive currents. Channel geometry and features that indicate subaerial exposure such as striated pavements, as well as glaciotectonic structures, are not observed in the studied succession. The concept of lodgment implies direct contact with the base of the glacier, where the sediments are subglacially deposited by active ice and are often deformed during the process of deposition and contain frequent inclusions of substratum (RuszczynH ska-Szenajch 2001).

FA5 is interpreted as offshore deposits without glacial influence (Fig. 10B). FA6 represents the progradation of a deltaic system formed by the sigmoidal lobe and distal mouth bars with the occurrence of *Arthrophycus*. FA6 was misunderstood by Janikian *et al.* (2019), who considered a “distal low slope braided river association” for strata belonging to the Ipu and Jaicós Formations. Trough cross-stratified sandstones of FA7 that represent the Jaicós Formation are interpreted as a fluvial system with the predominance of subaqueous dunes. In contrast to FA1, which is characterized by tabular beds, FA7 has lenticular sandstones indicating more channelized bodies.

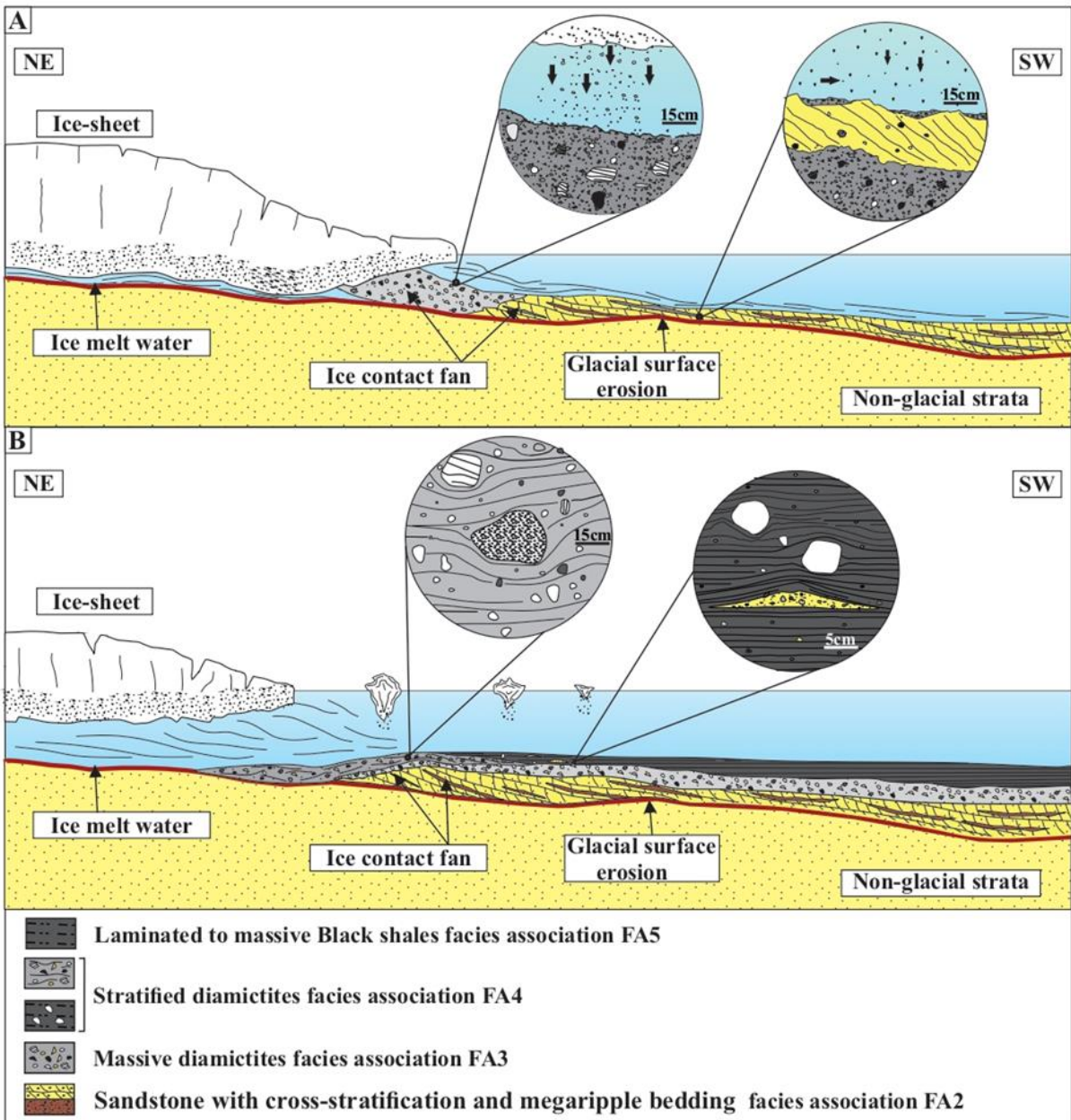


Figure 10. Simplified depositional model for the glacial record in the Serra Grande Group. A) During the ice sheet advance, deposits of massive diamicton by the ablation process were reworked by currents with migration of bedforms under partial suspension debris. B) Glacial retreat allowed the release of a large volume of meltwaters concomitant with gradual sea-level rise. In this phase, stratified diamictons were underlain by deposits of organic-rich muds initially influenced by ice-raftered debris coming from icebergs. The glacially influenced sea-level rise led to progressive long-term transgression.

3.6 SEQUENCE STRATIGRAPHY

Although the sedimentological data available to date (Assis *et al.* 2019, Barrera *et al.* 2018, Caputo & Lima 1984, Caputo & Santos 2019, Janikian *et al.* 2019) for the SGG indicate some components of depositional systems, these features still have not been properly integrated into a stratigraphic framework, which would enable us to perform an analysis of the evolving history based on sea-level changes. The stratigraphic charts formulated by Góes &

Feijó (1994) and Vaz *et al.* (2017), although they provide a lithostratigraphic framework, evoke second-order sequences that are of limited use for outcrop-based studies that generally involve third- and fourth-order sequences (Cateaneau 2019). This previous stratigraphy is valid mainly for the first three Paleozoic sequences generated during the tectonic stability of the Parnaíba Basin, with sequence boundaries related largely by the variations in sea level. The stratigraphic charts of Góes & Feijó (1994) and Vaz *et al.* (2007) are hybrid products formulated with some concepts of sequence stratigraphy but focused on a predominantly lithostratigraphic basis. In this work, the detailed mapping of parasequences and key surfaces in outcrops combined with the available chronostratigraphic data and their correlation with the global sea-level curve have improved the understanding of SGG sequence stratigraphy (Fig. 11). This new stratigraphic framework for the studied succession is compared with the proposal of Assis *et al.* (2019) to enhance knowledge about the Ordovician-Devonian events that occurred in West Gondwana (Fig. 11).

Glacial deposits are the main stratigraphic markers for the age of the studied succession. The possible Ordovician age for the glaciation in the Parnaíba Basin has been contested because the palynomorph content in the Serra Grande deposits more strongly indicates a Silurian age, particularly Llandoveryan as the probable age of glaciation for this part of West Gondwana (Grahn & Caputo 1992, Grahn *et al.* 2005, Le Hérisse *et al.* 2001). This age agrees with that found in the lower Paleozoic strata in the Amazon and Paraná basins that were tectonically connected with the Parnaíba Basin during the Silurian (Melo 1997, Melo & Steemans 1997, Milani *et al.* 2000, Mizusaki *et al.* 2002). However, the Silurian age for glaciogenic strata of the studied succession enables us to re-evaluate the age of preglacial and postglacial siliciclastic deposits even without the occurrence of age indicators such as palynomorphs or synsedimentary volcanic rocks (Fig. 11). We compare the recognition of depositional systems and systems tracts integrated into a stratigraphic framework based on the discontinuity surfaces according to lower Paleozoic sea-level changes (Fig. 11). In general, meter-scale cycles, shallowing-upward cycles and episodic (glaciogenic) deposits are the building blocks of the stratigraphic framework formed by three depositional sequences (Fig. 11). The analysis of the sequences considers the characterization of their boundaries according to subaerial exposure, erosion, alloogenetic events, modification of the stacking pattern of the cycles (progradational, retrogradational and aggradational) and abrupt facies changes (Fig. 11).

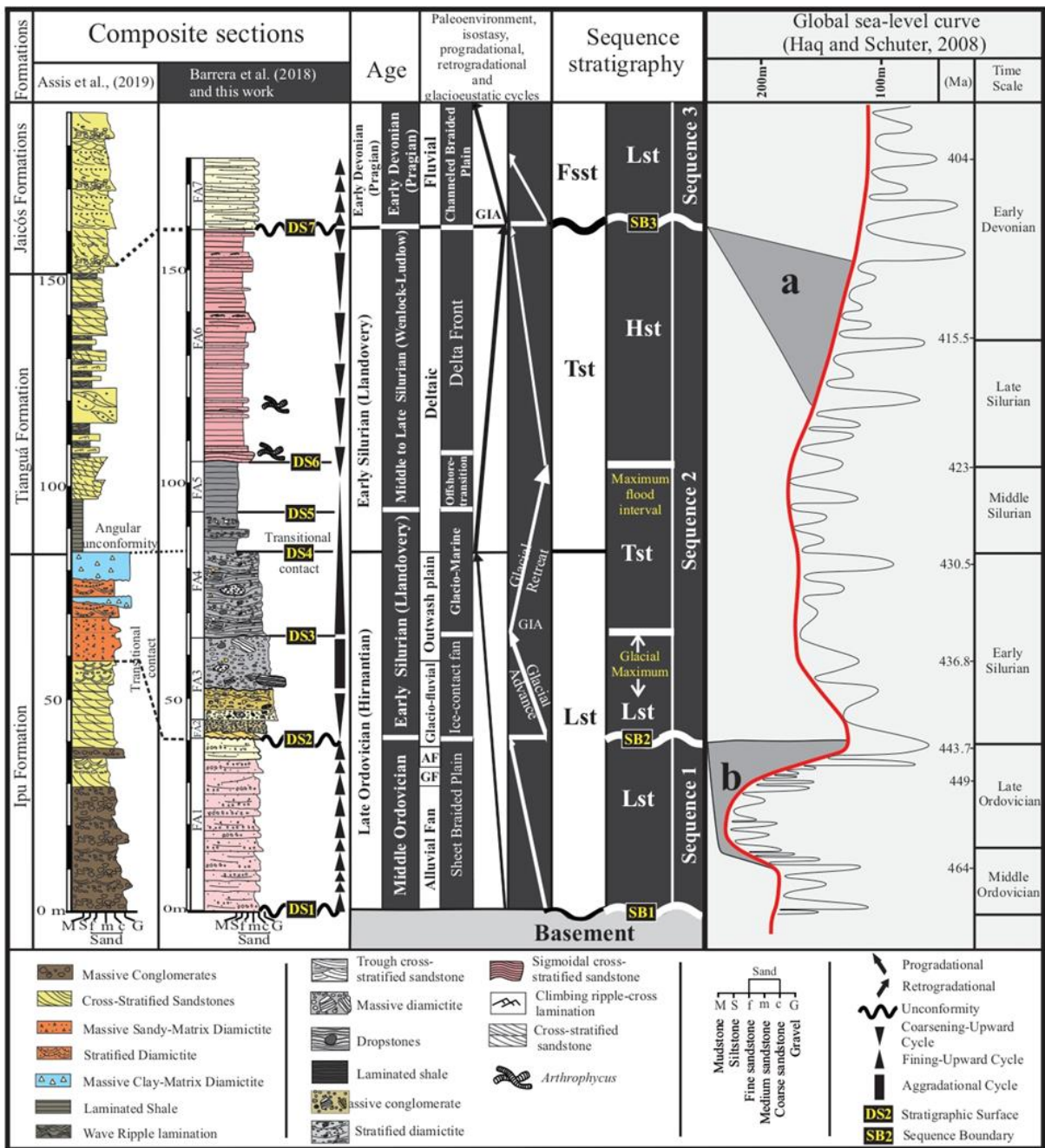


Figure 11. Stratigraphic analysis of the Ordovician-Devonian Serra Grande Group in the western Parnaíba Basin. Age, stacking patterns, paleoenvironment, and glacio-eustatic cycles are compared using the proposals of Assis *et al.* (2019), Barrera *et al.* (2018) and this work. Glacial deposits are used as stratigraphic markers to organize the age of succession based on paleontological data. The high-resolution stratigraphic data presented in this work allow correlations with the global relative sea-level curve for the lower Paleozoic and the age calibration of lithostratigraphic and systems tracts such as 1) the lower part of the Serra Grande Group previously interpreted as Late Ordovician and now repositioned in the Middle Ordovician; 2) the ice age previously considered Hirnantian and changed to Llandoveryan according to the age obtained in the Amazona and Paraná basins (Melo 1997, Melo & Steemans 1997, Mizusaki *et al.* 2002); and 3) the systems tracts and the nondeposition or erosive intervals (“a” and “b”) tentatively inferred following the curve inflection. Abbreviations: Lst, Lowstand systems tract; Fsst, Falling stage systems tract; Tst, Transgressive systems tract; Hst, Highstand systems tract; GIA, Glacio-isostatic adjustment; AF, Alluvial fan; GF, Glacio-fluvial.

3.6.1 Parasequences

A parasequence is a series of linked depositional systems. Each parasequence has different facies deposited within the same interval. The coastal parasequence described here may possibly have its equivalents in the updip (landward) portion or nonmarine environments. Marine to coastal parasequences where flooding surfaces juxtapose deeper-water facies over shallow-water deposits are relatively easy to identify; in contrast, the parasequence boundaries in continental facies are harder to recognize even if interpreted as distal successions, i.e., near-coastal facies. The incipient fining-upward cycles observed in FA1 (lower Ipu Formation) interpreted here as non-glaciogenic sheet braided deposits unrelated to overlying coastal deposits (FA2-FA6) are not considered parasequences (Fig. 11). This interpretation is different from that of Assis I. (2019), who considered a transition between fluvial deposits and glaciogenic sediments integrated in an outwash plain setting. The interpretation of these deposits as products of a pre-Silurian river deposited during lowstand conditions in the Ordovician is corroborated here. However, Assis *et al.* (2019) did not adequately explain why these deposits are positioned in the Upper Ordovician. Adjusting the lowstand interpretation with the global sea-level curve verifies that the extensive fall in sea level is more compatible with a Middle Ordovician age (Fig. 11).

The coarsening/fining-upward patterns observed in glacial deposits are related to ice sheet advance/retreat cycles (Ghienne *et al.* 2007, Le Heron *et al.* 2012) and are parasequences induced by glacio-eustasy. The stratified sandstone of FA2 is characterized by an overall upward increase in sediment grain size, which represents a progradational stacking pattern and the advance of the ice-sheet margin. This progradational basal series capped by massive diamictites (FA3) does not exhibit vertical grain-size variations and symbolizes an aggradational stacking pattern, which is a product of a quasi-stable ice-sheet margin. The massive diamictite beds are analogous to flow-till deposits and represent an episode of ice sheet advance followed by a still-stand. The upward transition to stratified diamictites and black shales (FA4) represents a retrogradational stacking pattern during the ice retreat phase. This stratigraphic stacking pattern coincides with sequence stratigraphic models developed explicitly for rapidly retreating ice sheets (cf. Ghienne *et al.* 2007). The glaciogenic succession is replaced upsection by coarsening-upward cycles of delta front and prodeltaic facies (FA5 and FA6) representative of progradational parasequences. This succession represents the transition between postglacial and long-term transgression conditions and is unconformably overlain by fluvial sediments (FA7).

3.6.2 Discontinuity surfaces

The analysis of individual outcrops was mainly focused on full mapping, recognizing key layers and discontinuity surfaces and inferring the possible genesis and stratigraphic significance (1 to 7; Fig. 11). The key surfaces for high-resolution sequence stratigraphic studies are stratigraphic contacts that help locate boundaries between sequences, as well as subdivide sequences into systems tracts (Zecchin & Catuneanu 2013). Three sequence boundaries (SB) and three other stratigraphic discontinuity surfaces (DSs) are recognized in the SGG record (Fig. 11).

DS1 represents an abrupt and irregular contact with the basement rocks of Borborema Province, representing a pronounced sequence boundary (SB1) and implying its formation during a long time of uplift succeeded by subsidence and formation of the basin and later by the deposition of FA1 (Figs. 1C, 11).

DS2 is the contact between sheet braided plain deposits (FA1) and glaciogenic sediments (FA2-FA4) interpreted as a pronounced basinal unconformity (SB2) related to a ravinement produced during the Ordovician-Silurian ice age. This surface developed during the maximum glacial period. Using the global sea-level curve to characterize the systems tract and the continuity of the stratigraphic record, we verify that only the lowstand succession (FA1) is preserved, while the retrogradational to progradational deposits have possibly been eroded (Fig. 11). Estimating the span of time in the succession is difficult because the siliciclastic nature of these deposits hinders obtaining a precise age. However, the estimate of age is tentatively made using the global sea-level curve that suggests an glacial erosion period of approximately 25 Myr (Fig. 11). Glacial erosion represents a simple mechanism when compared with subduction and uplift as factors to accelerate global erosion within the constraints of the sedimentary record (Keller *et al.* 2018, White 1973). Glaciers are unique erosive agents with the competence to modify the erosive base level, promoting continental denudation both directly through subglacial erosion and indirectly by the fall in the global base level when the continents are exposed to subaerial erosion (Keller *et al.* 2018). Modern glacial erosion rates considered in Greenland ice sheets are nearly two orders of magnitude faster than those registered for the Neoproterozoic glaciations estimated at approximately 0.0625 mm/y of substrate (Cowton *et al.* 2012). This scenario characterized by massive and thick ice sheets covering the substrate with limited or nonexistent accommodation space generated a low rate of sedimentation on the continent that bypassed deep waters below erosional base level (Keller *et al.* 2018).

DS3 is a glacio-eustatic transgressive surface linked to ice retreat and represents the postglacial early transgression. In this phase, the ocean was gradually exposed to the atmosphere, and the shedding of ice generated a series of icebergs that supplied debrites to the bottom of the sea (Fig. 10B). The lithostratigraphic contact between the Ipu and Tianguá Formations (DS4) was previously considered an angular unconformity formed by tectonic uplift due to the lack of glacial evidence (Fig. 11). In contrast, no tilting of beds is observed in the contact zone, and the presence of debrites in the black shales of the lower Tianguá Formation indicates a transitional contact, corroborating the observations of Barrera *et al.* (2018) and Janikian *et al.* (2019). DS5 is the flooding surface just above the glaciomarine deposits and represents the end of glacial influence and the beginning of the long-term transgression (TST in Fig. 11). DS6 is a transitional contact between the maximum flooding surface and the highstand phase (Fig. 11). DS7 between FA6 and FA7 is interpreted as a subaerial unconformity or a sequence boundary (SB3) due an accelerated sea-level fall that allowed the progradation of fluvial systems under deltaic deposits (FA6) suggestive of a delay in the tectono-eustatic cycle (see Johnson 1996).

3.6.3 Systems tracts and depositional sequences

The analysis of these deposits based on sea-level fluctuations and glacial influence enables the identification of the systems tracts inserted on three third-order depositional sequences (Seq) that can be sequenced in five evolutionary phases (Figs. 11 and 12). The mid-Ordovician sequence 1 (Seq1) is the lower portion of the Ipu Formation, which comprises only sheet braided plain deposits (FA1) and contains only the lowstand systems tract that was preserved as a record of glacial erosion, as discussed above (Fig. 12A and B). The Silurian Seq2 includes the upper portion of the Ipu and Tianguá Formations, which constitute glacial and deltaic deposits (Fig. 12C and D). The presence of glacial deposits in a stratigraphic succession affects the interpretations made from sequence stratigraphy. Therefore, adaptations are required to avoid misinterpretation of glacial and nonglacial records (Nutz *et al.* 2015). A sketch of the evolution of SGG depositional systems with a focus on glacio-eustatic cycles and sequence stratigraphy is shown in Fig. 11. During the course and end of the Ordovician-Silurian glacial event, factors such as glacio-eustatic sea-level changes and glacio-isostatic adjustment (GIA) controlled the accommodation space and morphology of the sedimentary bodies. Glacio-eustatic processes influence sea-level variations, as well as the morphology and distribution of proglacial sediments (Ghienne 2003). GIA controls the accommodation space during syn-deglacial stages, from the substrate response to the uplift of the land surface

following ice melt (Boulton 1990, Creveling & Mitrovica 2014, Whitehouse 2018, Zecchin *et al.* 2015). In contrast to this interpretation, Assis *et al.* (2019) proposed that the evolution of the SGG is composed of progradational (Ipu Formation) and retrogradational (Tianguá Formation) glacially influenced cycles and a nonglacial progradational cycle (Jaicós Formation) (influenced by GIA), all of which are separated by unconformities (Fig. 11). According to Assis *et al.* (2019), isostatic rebound occurs approximately 30 Ma after the end of the glacial event (Fig. 11). Postglacial isostatic rebound affecting the entire Serra Grande succession is difficult to understand, possibly because this event disturbed only the first meters of postglacial strata (Creveling and Mitrovica 2014, Whitehouse 2018). Seq3 is represented only by lowstand fluvial deposits (FA7) of the Jaicós Formation that unconformably overlie the highstand deposits of Seq2 and suggest long exposure of the coastal zone during sea-level fall (Figs. 11, 12E).

3.7 ORDOVICIAN-SILURIAN ICE AGE IN WEST GONDWANA

During the transition between the Ordovician and Silurian periods, western Gondwana was located in high southern latitudes, whereas its eastern portion was situated in equatorial latitudes with tropical conditions (Ghienne 2003). Paleogeographic reconstructions of the Late Ordovician glacial period typically show an ice-sheet center located near central Africa with the peripheral extent of the ice front remaining poorly known (Ghienne 2003, Torsvik & Cocks 2013). The timing of glaciation is still a matter of debate, mainly during the early Silurian (Díaz-Martínez & Grahn, 2007, Ghienne 2003). In agreement with paleontological data from ice distal and postglacial sedimentary successions, glacial sedimentation in northern Gondwana (Africa) has been restricted to the latest Ordovician, while in West Gondwana (South America), glacial sedimentation took place during the early Silurian (Brenchley *et al.* 1991, Díaz-Martínez & Grahn 2007, Leone *et al.* 1995, Zhang *et al.*, 2000).

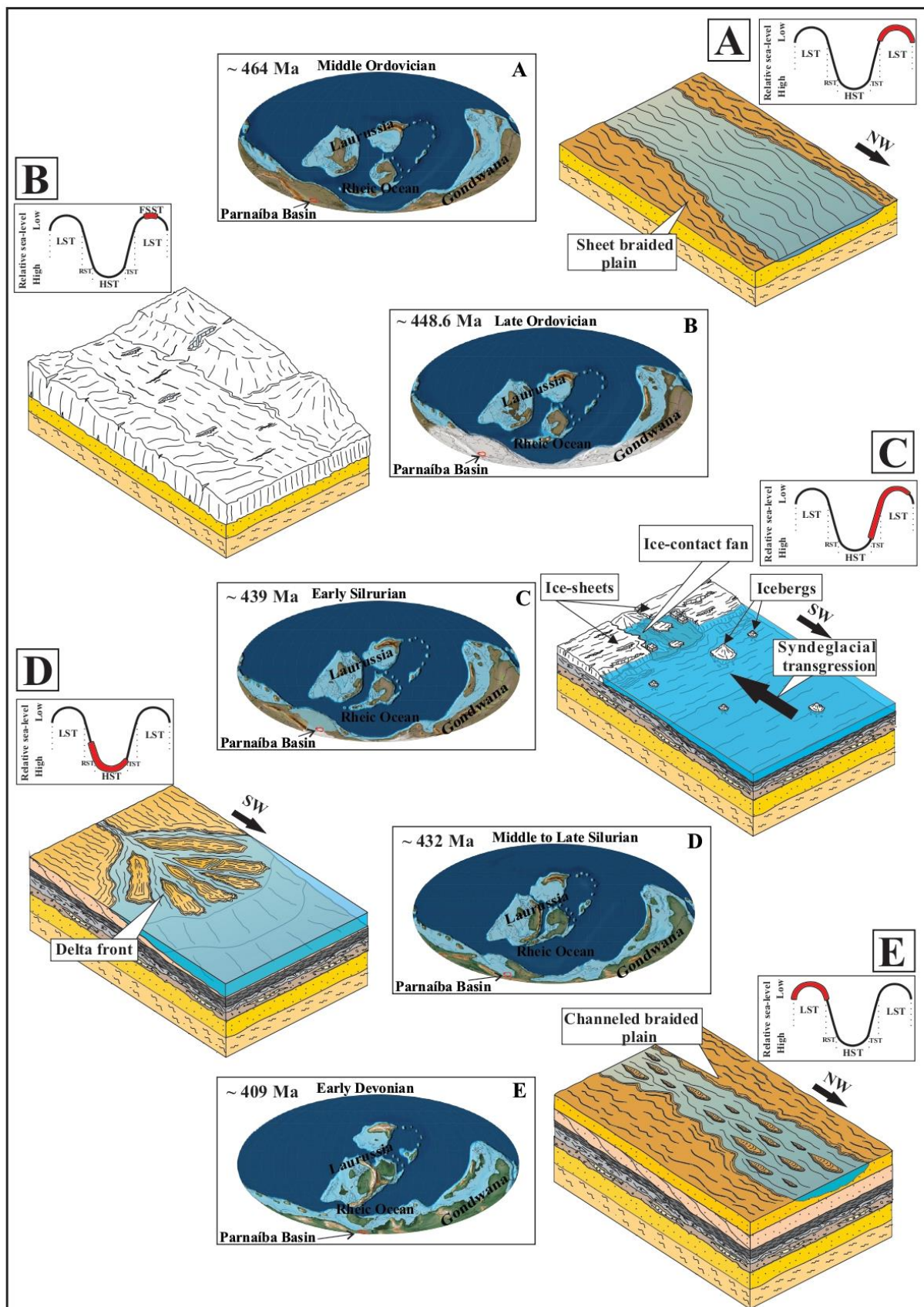


Figure 12. Sequential evolution of the Serra Grande Group in the eastern Parnaíba Basin. A) Middle Ordovician: the lowstand phase promoted the development of sheet braided deposits of Seq1 coming from southeastern Gondwana. B) Middle to Late Ordovician: the maximum glaciation promoted an extensive lowstand and massive erosion of substrate, totally removing the highstand and transgressive systems tracts of Seq1. C) Early Silurian: the lowstand phase of Seq2 was related to the advance of ice sheets in marginal areas of the basin, causing the deposition of ablation diamicton. The transgressive systems tract started during ice retreat and shedding of icebergs with pronounced deposition by ice rafted debris. D) Middle to late Silurian: the progressive sea-level rise and maximum flooding were accompanied by organic matter-rich mud in offshore settings, and subsequent progradation of a deltaic deposit marked the highstand phase. E) Early Devonian: an extensive sea-level fall renewed the continental drainage with the formation of a braided plain.

The glacial record present in northern Gondwana represents the glacial maximum of the Ordovician-Silurian ice age (Ghienne 2003). However, an ongoing discussion regards the precise age and paleoenvironmental interpretation of these deposits in South America. The age difference between these deposits generated during the same glacial event can be explained by the precise definition of the sedimentary environments and glacial processes. The Ordovician glacial deposits present in northern Gondwana represent sedimentation in front of the ice margin from continental glaciers in a non-confined environment that allowed deposition (Ghienne 2003). During this time interval, western Gondwana was characterized by thick glaciers covering the substrate with limited or nonexistent accommodation space, which generated a low rate of sedimentation on the continent that bypassed deep waters. This scenario does not allow the deposition or preservation of Ordovician deposits in Brazilian intracratonic basins. However, these deposits are recorded in deep water settings in the peripheral basins of Peru, Bolivia and Argentina (Díaz-Martínez & Grahn 2007).

3.8 CONCLUSIONS

The eastern Parnaíba Basin in northern Brazil is a highly favorable setting for studying episodes related to the Ordovician-Silurian glaciation. Previous studies in this region led to the recognition of unequivocally glaciogenic sediments associated with pre- and postglacial deposits, favoring the understanding of lower Paleozoic events that occurred in West Gondwana. Based on sedimentological, stratigraphic, and facies analyses supplemented by previous geological and geochronological data, some points about the Ordovician-Devonian sedimentary history of the eastern Parnaíba Basin are reinterpreted. The paleoenvironment of the SGG encompasses fluvial, glacial, and coastal facies, partially confirming the previous interpretation that, however, included the presence of a predominantly "subaerial" alluvial plain and outwash plain, which is completely discarded in our proposal. The proximal facies is incompatible with intermediary braided plain deposits, and subaerial features are not

observed in the studied succession, which is dominated by subaqueous settings. We refine the sequence stratigraphy of the SGG using facies and depositional system analyses, as well as a coherent interpretation of the key surfaces. In addition, the sedimentary succession is compared with the global sea-level curve to develop a more robust third-order sequential evolutionary model for these deposits. The sheet braided deposits (lower Ipu Formation) considered Middle Ordovician are unique lowstand sediments preserved in Sequence 1. If the transgressive and highstand strata of Sequence 1 were deposited, their removal by glacial dynamics probably occurred during the Late Ordovician to early Silurian, forming an extensive unconformity of approximately 25 Myr. A new sequence started with the advance of ice sheets into marginal areas of the basin, causing the deposition of ablation diamicton during the lowstand (upper Ipu Formation). The postglacial transgression is marked by ice rafted debris deposited from icebergs onto organic matter-rich mud (Tianguá Formation) in the shoreface-offshore zone. The maximum flooding in the middle to late Silurian was succeeded by a highstand phase marked by the progradation of deltaic deposits. Biological activity is marked by the presence of polychaetes that reworked the marine seafloor. In the Early Devonian, an extensive sea-level fall renewed the continental drainage with the formation of a braided plain (Jaicós Formation) marking the lowstand phase of Sequence 3.

The new interpretations presented here allow us to improve the correlation of these deposits with other successions worldwide and to understand the role of ice sheets and postglacial transgressions that affected West Gondwana during the Silurian period. Ongoing stratigraphic studies in the Parnaíba Basin to the same detail as those reported here for the SGG will potentially yield a more complete picture of the Ordovician-Devonian sedimentary record of West Gondwana.

Acknowledgments

We are very grateful to the National Council for Scientific and Technological Research (CNPq) for funding this research with a master scholarship (CNPq - 133509/2018-4) awarded to the first author, to the Programa de Pós-Graduação em Geologia e Geoquímica (PPGG) of the Federal University of Pará (UFPa) for logistic and financial support and to José Bandeira Junior for financial support from the CNPq project (460964/2014-3). We also thank Joelma Lobo for facilitating the production of thin sections and Afonso Quaresma, Andressa Nogueira and Sebastian Gomez for their logistic support; Werner Truckenbrodt, Ana Góes and Francisco Abrantes for his constructive comments on the manuscript.

CAPITULO IV CONSIDERAÇÕES FINAIS

As análises sedimentológicas e estratigráficas realizadas nos depósitos do Grupo Serra Grande na borda leste da Bacia do Parnaíba, revelaram a evolução espacial e temporal de sistemas fluviais, glaciais e costeiros. Este registro estratigráfico foi agrupado em sete associações de fácies (AF). A associação de fácies arenitos tabulares com estratificação cruzada (AF1) representa a instalação de um extenso sistema fluvial, localizado diretamente sobre o embasamento da bacia. Arenitos e conglomerados com espessuras de centenas de metros que compõem esse registro sugerem deposição a partir de um rio perene provavelmente suprido por regiões montanhosas ao Oeste do Gondwana. A FA1 é truncada no topo por uma superfície de erosão glacial, produzida pelo avanço e retrabalhamento do substrato por parte das geleiras. O registro glacial começou após o desenvolvimento desta superfície erosiva, composta pelas associações de fácies AF2, AF3 e AF4. A estreita associação entre processos de tração, fluxo de detritos e depósitos *ice rafted debris* indica uma origem subaquática para essas rochas. O fim do evento glacial está representado pela AF5. Posteriormente, a progradação de um sistema deltaico (AF6) marca o início de um novo período de queda do nível do mar. Nas porções basais da AF6, foram identificadas ocorrências do icnogênero *Arthrophycus*, reafirmando o caráter marinho do corpo de água onde ocorreu a deposição desses sedimentos. A transição entre as associações de fácies AF6 e AF7 estão representadas por uma superfície erosiva produto de uma queda acelerada do nível do mar que permitiu a progradação de sistemas fluviais (AF7).

Esta proposta confirma parcialmente interpretações paleoambientais previas, descartando a presença depósitos gerados em leques aluviais e *outwash plains*. A estratigrafia de sequências do Grupo Serra Grande foi refinada usando principalmente a interpretação coerente das superfícies chave e correlacionando os tratos de sistema com a curva global do nível do mar, fornecendo um modelo evolutivo sequencial de terceira ordem mais robusto que inclui três sequências deposicionais. A AF1 localizada diretamente sobre o embasamento cristalino representa depósitos gerados dentro de condições de mar baixo pertencentes à sequência 1, possivelmente durante o Ordoviciano Médio. Estes depósitos são truncados por uma expressiva inconformidade de origem glacial que provavelmente removeu os estratos gerados em condições transgressivas e de mar alto. Essa inconformidade produzida pela dinâmica glacial retirou aproximadamente 25 Ma do registro sedimentar da bacia. A segunda sequência iniciou com o avanço das geleiras no Siluriano Inferior, a partir da instalação de um

ice-contact fan (AF2 e AF3), em condições de mar baixo. Durante o recuo das geleiras grandes quantidades de água e detritos foram liberados permitindo a deposição de diamictitos estratificados com presença de clastos caídos (AF4). A fase de desgelo culminou no aumento do nível do mar e posterior deposição de folhelhos negros da AF5, possivelmente durante o Siluriano médio a tardio. A fase de mar alto no Siluriano tardio é marcada instalação de um sistema deltaico (AF6). No Devoniano inferior uma nova expressiva etapa de descida do nível do mar produziu uma discordância na plataforma concomitante com a progradação de sistemas fluviais entrelaçados (AF7), em condições de mar baixo pertencentes à sequência 3.

A sucessão sedimentar descrita para o Grupo Serra Grande representa o registro da primeira glaciação paleozoica no Continente Sul-Americano. Adicionalmente, dentro dessas rochas foram identificadas evidências, do aumento mais significativo no nível eustático do mar registrado na história da Terra. As novas interpretações apresentadas neste trabalho permitiram entender o papel dos lençóis de gelo e das transgressões pós-glaciais que afetaram o Gondwana Oeste durante o Siluriano.

REFERÊNCIAS

- Adôrno R. R. 2014. *Estudo cronobioestratigráfico da Formação Vila Maria: litoestratigrafia e paleontologia do limite ordoviciano-siluriano da Bacia do Paraná, estados de Goiás e de Mato Grosso, Brasil central.* MS Dissertation, Instituto de Geociências, Universidade de Brasília, Brasília. 94.
- Assine M.L., Alvarenga C.J.S., Perinotto J.A.J. 1998. Formação Iapó: glaciação continental no limite Ordoviciano/Siluriano da Bacia do Paraná. *Revista Brasileira de Geociências*, **28**(1): 51-60.
- Assis A.P., Porto A.L., Schmitt R.S., Linol B., Medeiros S.R., Correa Martins F., Silva D.S. 2019. The Ordovician-Silurian tectono-stratigraphic evolution and paleogeography of eastern Parnaíba Basin, NE Brazil. *Journal of South American Earth Sciences*, **95**: 102241. Doi: <https://doi.org/10.1016/j.jsames.2019>.
- Barrera I.A., Nogueira A.C., Bandeira J.C., Neita J.S., Nogueira A.A. 2018. a primeira ocorrência do icnogênero arthropycus em depósitos silurianos da bacia do parnaíba, região de Ipueiras, Ceará. *Boletim do Museu de Geociências da Amazônia*, **5**: 1-7. Doi: <https://doi.org/10.31419/ISSN.2594-942X.v52018i3a7IARB>.
- Bhattacharya J.P. 2006. "Deltas". In: Posamentier H.W. & Walker R.G. (eds.). *Facies models revisited*. SEPM Society for Sedimentary Geology. 237-293.
- Boulton G.S. & Deynoux M. 1981. Sedimentation in glacial environments and the identification of tills and tillites in ancient sedimentary sequences. *Precambrian Res.*, **15**: 397–422. Doi: [https://doi.org/10.1016/0301-9268\(81\)90059-0](https://doi.org/10.1016/0301-9268(81)90059-0).
- Boulton G.S. 1990. Sedimentary and sea level changes during glacial cycles and their control on glacimarine facies architecture. In: Dowdeswell J.A. & Scourse J.D. (eds.). *Glacimarine environments: processes and sediments*. 15-52. Special Publication. (v. **53**. *Geological Society, London*).
- Boyce J.I. & Eyles N. 2000. Architectural element analysis applied to glacial deposits: internal geometry of a late Pleistocene till sheet, Ontario, Canada. *Geological Society of America Bulletin*. **112**: 98–118.
- Brenchley P.J., Romano M., Young T.P., Storch P. 1991. Hirnantian glaciomarine diamictites evidence for the spread of glaciation and its effect on Upper Ordovician faunas. In: Barnes C.R. & Williams S.H. (eds.). *Advances in ordovician geology*. [Cambridge], Cambridge University Press. 325-336. (*Geol. Surv. Can. Pap.* 90-9).
- Brenchley P.J., Marshall J.D., Carden G.A.F., Robertson D.B.R., Long D.G.F., Meidla T., Hints L., Anderson T.F. 1994. Bathymetric and isotopic evidence for a shortlived Late Ordovician glaciation in a greenhouse period. *Geology*, **22**: 295-298.

- Brenchley P.J., Carden G.A., Hints L., Kaljo D., Marshall J.D., Martma T., Meidla T., Nõlvak J. 2003. High-resolution stable isotope stratigraphy of Upper Ordovician sequences: constraints on the timing of bioevents and environmental changes associated with mass extinction and glaciation. *GSA Bulletin*. **115** (1): 89–104. Doi: [https://doi.org/10.1130/0016-7606\(2003\)115<0089:HRSISO>2.0.CO;2](https://doi.org/10.1130/0016-7606(2003)115<0089:HRSISO>2.0.CO;2).
- Brito Neves B.B., Fuck R.A., Cordani U.G., Thomaz F. A. 1984. Influence of basement structures on the evolution of the major sedimentary basins of Brazil: a case of tectonic heritage. *J. Geodyn.* **1**: 495–510. Doi: [https://doi.org/10.1016/0264-3707\(84\)90021-8](https://doi.org/10.1016/0264-3707(84)90021-8).
- Brunt K., Fricker H., Padman L. 2011. Analysis of ice plains of the Filchner–Ronne Ice Shelf, Antarctica, using ICESat laser altimetry. *Journal of Glaciology*, **57**(205): 965-975. Doi: <https://doi.org/10.3189/002214311798043753>
- Campbell D.F. 1949. *Revised report on the reconnaissance geology of the Maranhão basin*. Rio de Janeiro, Brasil, Conselho Nacional do Petróleo. (Relatório Interno, 117 p.). (PETROBRAS - Sistema de Informação em Exploração - SIEX 103-0093).
- Caputo M.V. 1984. *Stratigraphy, tectonics, paleoclimatology and paleogeography of Northern basins of Brazil*. Phd Thesis, Universidade da California, Santa Barbara. USA. 603.
- Caputo M.V. & Lima E.C. 1984. Estratigrafia, idade e correlação do Grupo Serra Grande-Bacia do Parnaíba. In: SBG, *Anais do XXXIII, 33º Congresso Brasileiro de Geologia, Rio De Janeiro*. **11**. 228–241.
- Caputo M. V. & Dos Santos R. O. 2019. Stratigraphy and ages of four Early Silurian through Late Devonian, Early and Middle Mississippian glaciation events in the Parnaíba Basin and adjacent areas, NE Brazil. *Earth-Science Reviews*. 103002.
- Carozzi A.V., Falkenhein F.U.M., Carneiro R.G., Esteves R.P., Contreiras C.J.A. 1975. *Análise ambiental e evolução tectônica sinsedimentar da seção siluro-eocarbonífera da Bacia do Maranhão*. Rio de Janeiro, Brasil, Petrobras, 48 . (Série Ciência-Técnica-Petróleo. Seção Exploração de Petróleo n. 7).
- Catuneanu O. 2019. Scale in sequence stratigraphy. *Marine and Petroleum Geology*, **106**: 128-159.
- Cheel R.J. & Rust B.R. 1986. A sequence of soft-sediment deformation (dewatering) structures in late Quaternary subaqueous outwash near Ottawa, Canada. *Sediment. Geol.* **47**: 77–93.
- Christie-blick N., Dyson I.A., Von der borch C.C. 1995. Sequence stratigraphy and the interpretation of Neoproterozoic earth history: *Precambrian Research*. **73**: 3–26.
- Church M. & Gilbert R. 1975. Proglacial fluvial and lacustrine environments. In: Jopling A.V. & McDonald B.C. (eds.). *Glaciofluvial and glaciolacustrine sedimentation*. Ontario, Soc. Econ. Paleontol. Mineral., Spec. Publ. **23**. 22–100. (Special Publication, **23**).

- Cotter E. 1978. The evolution of fluvial style, with special reference to the Central Appalachian Paleozoic. In: Miall A.D. (eds.). *Fluvial sedimentology: Canadian Society of Petroleum Geologists. Canada. Memoir 5*. 361–383.
- Cowton T., Nienow P., Bartholomew I., Sole A., Mair D. 2012. Rapid erosion beneath the Greenland ice sheet. *Geology*. **40**: 343–346.
- Creveling J. R. & Mitrovica J. X., 2014. The sea-level fingerprint of a Snowball Earth deglaciation: *Earth Planet Sci. Lett.* **399**: 74–85.
- Daly M.C., Andrade V., Barousse C.A., Costa R., McDowell K., Piggott N., Poole A.J. 2014. Brasiliano crustal structure and the tectonic setting of the Parnaíba basin of NE Brazil: results of a deep seismic reflection profile. *Tectonics*. **33**: 2102–2120.
- Davies N.S., Gibling M.R., Rygel M.C. 2011. Alluvial facies evolution during the Palaeozoic greening of the continents: case studies, conceptual models and modern analogues. *Sedimentology*. **58**: 220–258.
- De Castro D.L., Fuck R.A., Phillips J.D., Vidotti R.M., Bezerra F.H.R., Dantas E.L. 2014. Crustal structure beneath the Paleozoic Parnaiba Basin revealed by airborne gravity and magnetic data. Brazil. *Tectonophysics*. **614**: 128–145. Doi: <https://doi.org/10.1016/j.tecto.2013.12.009>.
- Deynoux M. 1985. Terrestrial or waterlain glacial diamictites? Three case studies from the Late Precambrian and Late Ordovician glacial drifts in West Africa. *Palaeogeogr. Palaeoclimatol. Palaeoecol.* **51**: 97–141.
- Díaz-Martínez, E. 1997a. Facies y ambientes sedimentarios de la Formación Cancañiri (Silúrico inferior) en La Cumbre de La Paz, norte de la Cordillera Oriental de Bolivia. *Geogaceta*. **22**: 55–57.
- Díaz-Martínez, E. 1998. Silurian of Peru and Bolivia: recent advances and future research. 6th International Graptolite Conference and Field Meeting of the International Subcommission on Silurian Stratigraphy, Madrid. *Temas Geológico-Mineros del Instituto Tecnológico Geominero de España*. **23**: 69–75.
- Díaz-Martínez E., Acosta H., Cárdenas J., Carlotto V., Rodríguez R. 2001. Paleozoic diamictites in the Peruvian Altiplano: evidence and tectonic implications. *Journal of South American Earth Sciences*. **14**: 587–592.
- Díaz-Martínez E. & Grahn Y. 2006. Early Silurian glaciation along the western margin of Gondwana (Peru, Bolivia and northern Argentina): Paleogeographic and geodynamic setting. *Paleogeography, Paleoclimatology, Paleoecology*. **245**: 62–81.
- Eyles N. 1993. Earth's glacial record and its tectonic setting. *Earth-Science Reviews*. **35**: 1–248.
- Frakes L.A., Francis J.E., Syktus J.I. 1992. Climate modes of the Phanerozoic. Cambridge, Cambridge University press.

- Galehouse J. S. 1971. Sedimentation analysis. In: Procedures in sedimentary petrology; (eds) Carver R. E., New York: Wiley-Interscience. 65–94.
- Galloway W. 1975. Process framework for describing the morphologic and stratigraphic evolution of deltaic depositional system. *Society of Economic Paleontologists and Mineralogist (SEPM), Special Publication*. **31**: 127–156.
- Ghienne J.-F. 2003. Late Ordovician sedimentary environments, glacial cycles, and post-glacial transgression in the Taoudeni Basin, West Africa. *Palaeogeography, Palaeoclimatology, Palaeoecology*. **189**: 117–145.
- Ghienne J.-F., Le Heron D., Moreau J., Denis M., Deynoux M. 2007. The Late Ordovician glacial sedimentary system of the North Gondwana platform. In: Hambrey, M., Christoffersen, P., Glasser, N., Janssen, P., Hubbard, B., Siegert, M. (Eds.), *Glacial Sedimentary Processes and Products*. Special Publication. International Association of Sedimentologists. **39**: 295–319.
- Gibling M.R., Davies N.S., Falcon-Lang H.J., Bashforth A.R., Di Michele W.A., Rygel M.C., Ielpi A. 2014. Palaeozoic co-evolution of rivers and vegetation: a synthesis of current knowledge. *Proc. Geol. Assoc.* **125**: 524–533.
- Góes A.M.O., Souza J.M.P., Teixeira L.B. 1990. Estágio Exploratório e Perspectivas Petrolíferas da Bacia do Parnaíba. *Bol. Geociencias Petrobras* **4**: 55–64.
- Góes A.M.O., Travassos W.A., Nunes K.C. 1992. *Projeto Parnaíba – reavaliação da bacia e perspectivas exploratórias*. Belém, PETROBRAS. Rel. interno.
- Góes A.M.O. & Feijó F.J. 1994. *Bacia do parnaíba*. Bol. Geociencias Petrobras. **8**: 57–67.
- Grahn Y. & Caputo M.V. 1992. Early Silurian glaciations in Brazil. *Palaeogeography, Palaeoclimatology, Palaeoecology*. **99**: 9–15.
- Grahn Y. & Gutiérrez P. 2001. Silurian and Middle Devonian chitinozoa from the Zapla and Santa Bárbara Ranges, Tarija Basin, northwestern Argentina. *Ameghiniana*. **38**: 35–50.
- Grahn Y. & De Melo J.H.G., Steemans A.P. 2005. Integrated chitinozoan and miospore zonation of the Serra Grande group (Silurian-Lower devonian), Parnaíba Basin, northeast Brazil. *Rev. Espanola Micropaleontol.* **37**: 183–204.
- Häntzschel W. 1975. Trace fossils and problematica. In: Teichert C. (ed.) Treatise on Invertebrate paleontology, Boulder, University of Kansas Press. 177–243.
- Haq B.U. & Schutter S.R. 2008. A chronology of Paleozoic sea-level changes. *Science*. **322**: 64–68.
- Hart J.K. & Roberts D.H. 1994. Criteria to distinguish between subglacial glaciotectonic and glaciomarine sedimentation. I. Deformational styles and sedimentology . *Sedimentary Geology*. **91**: 191–214.

- Hjellbakk A. 1997. Facies and fluvial architecture of a high-energy braided river: the Upper Proterozoic Segladden Member, Varanger Peninsula, northern Norway. *Sedimentary Geology*. **114**: 131-161.
- Hornung J.J., Asprion U., Winsemann J. 2007. Jet efflux deposits of a subaqueous ice contact fan, glacial Lake Rinteln, northwestern Germany. *Sed. Geol.*, **193**: 167–192.
- Ielpi A. & Rainbird R. 2015. Architecture and morphodynamics of a 1.6 Ga fluvial sandstone: Ellice Formation of Elu Basin, Arctic Canada. *Sedimentology*. **62**: 1950-1977. Doi: <https://doi.org/10.1111/sed.12211>.
- Ingram R.L. 1954. Terminology for the thickness of stratification and parting units in sedimentary rocks. *Geology Society Bulletin*. **65**: 937-938.
- Janikian L., Almeida R., Galeazzi C., Tamura L., Ardito J., Chamani M. 2019. Variability of fluvial architecture in a poorly vegetated Earth: Silurian sheet-braided and meandering ancestor river deposits recorded in northeastern Brazil. *Terra Nova*. Doi: <https://doi.org/10.1111/ter.12446>.
- Johnson M.E. 1996. Stable cratonic sequences and a standard for Silurian eustasy. *Geol. Soc. Am. Spec. Pap.* **306**: 203-211.
- Kegel W. 1953. *Contribuição para o estudo do Devoniano da Bacia do Parnaíba*. Rio de Janeiro, Brazil, Departamento Nacional da Produção Mineral, Divisão de Geologia e Mineralogia, Boletim no. 135. 38 .
- Keller C.B., Husson J.M., Mitchell R.N., Bottke W.F., Germon T.M., Boehnke P., Bell E.A., Swanson-Hysell N.L., Peters S. 2018. Neoproterozoic glacial origin of the Great Unconformity. *PNAS* **116** (4), 1136–1145.
- Kerans C. & Tinker S.W. 1997. Sequence stratigraphy and characterization of carbonate reservoirs: SEPM (*Society of Sedimentary Geology*) Short Course Notes No. **40**, 130.
- Larsson, R., 1991. Geological consequences of super-plumes. *Geology*. **19**: 963–966.
- Le Hérissé, A., Melo, J.H.G., Quadros, L.P., Grahn, Y., Steemans, P., 2001. Palynological characterization and dating of the Tianguá Formation, Serra Grande Group, northern Brazil. In: Melo, J.H.G., Terra, G.J.S. (Eds.), Correlação de Seqüências Paleozóicas Sul-Americanas. *Ciência-Técnica-Petróleo*. **20**: 25–41.
- Le Heron D., Busfield M., Kamona F. 2012. An interglacial on snowball Earth? Dynamic ice behaviour revealed in the Chuos Formation, Namibia. *Sedimentology*. **60**: 411-427. Doi: <https://doi.org/10.1111/j.1365-3091.2012.01346.x>.
- Leone F., Loi A., Pillola G.L. 1995. The post-sardic Ordovician sequence in south-western Sardinia. Guide Book, 6th Paleobenthos International Symposium: *Rend. Sem. Fac. Sc. Univ. Cagliari, suppl.* **65**. 81–106.

- Linol B., de Wit M.J., Barton E., de Wit M.M.J.C., Guillocheau F. 2016a. U-Pb detrital zircon dates and source provenance analysis of Phanerozoic sequences of the Congo Basin, central Gondwana. *Gondwana Res.* **29**: 208–219. Doi: <https://doi.org/10.1016/j.gr.2014.11.009>.
- Linol B., Wit M.J. De, Kasanzu C.H., Schmitt S., Corrêa-martins F.J., Assis A.P. 2016b. Origin and Evolution of the Cape Mountains and Karoo Basin. Switzerland: *Springer Nature*. 183–192. Doi: <https://doi.org/10.1007/978-3-319-40859-0>.
- Lønne, I., 1995. Sedimentary facies and depositional architecture of ice-contact glaciomarine systems. *Sediment. Geol.* **98**: 13–43.
- Long D.G.F. 1978. Proterozoic stream deposits: some problems of recognition and interpretation of ancient sandy fluvial systems. In: Miall, A.D. (Ed.), Fluvial Sedimentology. *Can. Soc. Pet. Geol., Mem.* **5**. 313–341.
- Lowe D. 2006. Water escape structures in coarse grained sediment. *Sedimentology*. **22**. 157 - 204. Doi: <https://doi.org/10.1111/j.1365-3091.1975.tb00290.x>.
- McDonald B.C. & Vincent J.S. 1972. Fluvial sedimentary structures formed experimentally in a pipe, and their implications for interpretation of subglacial sedimentary environments: *Geological Survey of Canada*. 72–27, 30.
- McDougall N. & Martin M. 2000. Facies models and sequence stratigraphy of Upper Ordovician outcrops in the Murzuq Basin, SW Libya. In: Sola M.A., Worsley D. (Eds.), Geological Exploration in Murzuq Basin. *Elsevier Science*. 223–236.
- Melchin M. J., Sadler P. M., Cramer B. D. 2012. The Silurian Period. With contributions by R. Cooper, O. Hammer and F. M. Gradstein. In: Gradstein F. M., Ogg J. G., Schmitz M., Ogg G. et al. (Eds.). *The Geological Time Scale*. Elsevier. 525–59.
- Melo J.H.G. 1997. *Resultados de solicitação de análise palinológica em amostras de superfície da região da represa Balbina (AM), Bacia do Amazonas*. Comunicação técnica SEBIPE 10/97. Petrobrás. (Relatório interno).
- Melo J.H.G. & Steemans P. 1997. *Resultados de investigações palinoestratigráficas em amostras de superfície da região de Presidente Figueiredo (AM), Bacia do Amazonas*. Comunicação técnica SEBIPE 048/97. Petrobrás. (Relatório interno).
- Menzies J., van der Meer J.J.M., Ravier E. 2016. A Kinematic Unifying Theory of Microstructures in Subglacial Tills. *Sedimentary Geology*. **344**: 57-70. Doi: <https://doi.org/10.1016/j.sedgeo.2016.03.024>.
- Metelo C.M.S. 1999. Caracterização estratigráfica do Grupo Serra Grande (Siluriano) na borda sudeste da Bacia do Parnaíba. MS Dissertation. Universidade Federal do Rio de Janeiro, Rio Janeiro, Brasil. 102. Doi: <http://objdig.ufrj.br/10/dissert/513062.pdf>.
- Miall A.D. 1981. Analysis of fluvial depositional systems. Education Course Note Series. *American Association of Petroleum Geologists*. **20**:1-75.

- Milani E.J. & Thomaz-Filho A. 2000. *Sedimentary basins of South America*. In: Cordani U. G., Milani E. J., Thomaz-Filho A., Campos D. A. (eds). *Tectonic evolution of South America*. Rio de Janeiro, Academia Brasileira de Ciências e Departamento Nacional da Produção Mineral (DNPM), 31st International Geological Congress. p. 389–449.
- Miller J.G.M. 1996. Glacial sediments. In: Reading H.G. (eds.). *Sedimentary environments: processes, facies and stratigraphy*. 3rd ed. [S.l], published by Wiley. 454-483.
- Mizusaki A.M.P., Melo J.H.G., Vignol-Lelarge M.L., Steemans P. 2002. Vila Maria Formation (Silurian, Paraná Basin, Brazil): integrated radiometric and palynological age determinations. *Geological Magazine*. **139** (4): 453–463. Doi: <https://doi.org/10.1017/S0016756802006659>
- Munnecke A., Calner M., Harper D., Servais T. 2010. Ordovician and Silurian sea–water chemistry, sea level, and climate: A synopsis. *Palaeogeography, Palaeoclimatology, Palaeoecology*. **296**: 389-413. Doi: <https://doi.org/10.1016/j.palaeo.2010.08.001>.
- Müller R.D., Sdrolias M., Gaina C., Steinberger B., Heine C. 2008. Long-term sea-level fluctuations driven by ocean basin dynamics. *Science*. **319**: 1357–1362.
- Mutti E., Tinterri R., Benevelli G., Di Biase D., Cavanna G. 2003. Deltaic, mixed and turbidite sedimentation of ancient foreland basins. *Marine and Petroleum Geology*. **20**: 733-755.
- Nutz A., Ghienne J.-F., Schuster M., Dietrich P., Roquin C., Hay M.B., Bouchette F., Cousineau P.A. 2015. Forced regressive deposits of a deglaciation sequence: example from the Late Quaternary succession in the Lake Saint-Jeanbasin (Quebec, Canada). *Sedimentology*. Doi: <http://dx.doi.org/10.1111/sed.12196>.
- Ó Cofaigh C., Dowdeswell J.A., Allen C.S., Hiemstra J.F., Pudsey C.J., Evans J., Evans D.J.A. 2005. Flow dynamics and till genesis associated with a marine-based Antarctic palaeo-ice stream. *Quaternary Science Reviews*, **24**: 709–740.
- Olariu C. & Bhattacharya J.P. 2006. Terminal distributary channels and delta front architecture of river-dominated delta systems. *Journal of Sedimentary Research*. **76**(2): 212-233.
- Oliveira D.C. & Mohriak W.U. 2003. Jaibaras trough: an important element in the early tectonic evolution of the Parnaíba interior sag basin, Northern Brazil. *Mar. Pet. Geol.* **20**: 351–383. Doi: [https://doi.org/10.1016/S0264-8172\(03\)00044-8](https://doi.org/10.1016/S0264-8172(03)00044-8).
- Owen Geraint. 2003. Load structures: Gravity-driven sediment mobilization in the shallow subsurface. *Geological Society, London, Special Publications*. **216**: 21-34. Doi: <https://doi.org/10.1144/GSL.SP.2003.216.01.03>.
- Plummer P.D. 1946. *Geossinclíneo do Parnaíba*. In: *Conselho Nacional do Petróleo*. Relatório de 1946. Rio de Janeiro, 1948. 87-134. (PETROBRAS).

Porto A., Daly M.C., La Terra E., Fontes S.L. 2018. The pre-Silurian Riachão Basin: a new perspective on the basement of the Parnaíba Basin, NE Brazil. Cratonic basin form. A case study Parnaíba basin Brazil. *Geological Society of London, Special Publications* **472**. SP472-2. Doi: <https://doi.org/10.1144/SP472.2>.

Powell R.D. 1990. Glacimarine processes at grounding-line fans and their growth to ice-contact deltas. In: Dowdeswell J.A. & Scourse J.D. (ed.). *Glacimarine environments: processes and Sediments*. [S.l., s.n] p.53–73. (Geol. Soc. London Spec. Publ. n. 53).

Ravier E., Buoncristiani J-F., Clerc S., Guiraud M., Menzies J., Portier E. 2014. Sedimentological and deformational criteria for discriminating subglaciofluvial deposits from subaqueous ice-contact fan deposits: a Pleistocene example (Ireland). *Sedimentology*. **61**: Doi: <https://doi.org/10.1111/sed.12111>.

Reading H.G. & Collison J.D. 1996. Clastic coast. In: Reading H.G. (eds.). *Sedimentary environments: processes, facies and stratigraphy*. 3rd ed. [S.l.] published by Wiley. 154-228.

Rodrigo L.A., Castaños A., Carrasco R. 1977. La formación cancañiri: sedimentología y paleogeografía. *Revista de Geociencias de la Universidad Mayor de San Andrés*. **1**: 1–22.

Rodrigues R. 1967. *Estudo sedimentológico e estratigráfico dos depósitos silurianos e devonianos da Bacia do Parnaíba*. PETROBRAS. RENOR, Belém, Brasil, Relatório Interno no 273M.

Røe S. 1987. Cross-strata and bedforms of probable transitional dune to upperstage plane bed origin from Late Pre-Cambrian fluvial sandstone, northern Norway. *Sedimentology*. **34**: 89-101.

Russell H.A.J. & Arnott R.W.C. 2003. Hydraulic-jump and hyperconcentrated-flow deposits of a glacigenic subaqueous fan: oak ridges moraine, Southern Ontario, Canada. *J. Sediment. Res.* **73**: 887–905.

Ruszczyńska-Szenajch H. 2001. “Lodgement till” and “deformation till”. *Quaternary Science Reviews*. **20**: 579–581. Doi: [https://doi.org/10.1016/S0277-3791\(00\)00097-4](https://doi.org/10.1016/S0277-3791(00)00097-4).

Sarg JF. 1988. Carbonate sequence stratigraphy. See Wilgus *et al.* 1988. 155-81.

Schumm S. A. 1968. Speculations concerning paleohydrologic controls of terrestrial sedimentation. *Geol. Soc. Am. Bull.* **79**: 1573-1588.

Scotese C.R. 2014. Atlas of Silurian and Middle-Late Ordovician Paleogeographic Maps (Mollweide Projection), Maps 73 – 80, Volumes 5, The Early Paleozoic, PALEOMAP Atlas for ArcGIS, PALEOMAP Project, Evanston, IL.

Scotese C.R. 2015. The ultimate plate tectonic flipbook, *Rob Van der voo retirement symposium*. Department of Earth and Environmental Sciences, University of Michigan, Ann Arbor, MI, August 26-27.

Scotese C. 2016. *Some thoughts on global climate change*: the transition from icehouse to hothouse. PALEOMAP Project, 21a, 1–2. University of Texas, Arlington, TX.

- Small H.L. 1914. *Geologia e suprimento de água subterrânea no Piauí e parte do Ceará.* Inspect. Obras contra secas. 137. (Ser. I.D., 32).
- Smith D.G. 1976. Effect of vegetation on lateral migration of anastomosed channels of a glacier meltwater river. *Geological Society of America Bulletin*, **87**: 857-860.
- Soares E. A. A. 1998. *Fácies litorâneas glaciais da formação Nhamundá (Siluriano inferior), na região de Presidente Figueiredo, AM, Bacia do Amazonas.* MS Dissertation, Centro de Geociências, Universidade Federal do Pará, Belém.
- Stronge W. B., Diaz H. F., Bokuniewicz H., Inman D. L., Jenkins S. A., Hsu J. R. C., Scheffers A. 2005. Europe, coastal geomorphology. *Encyclopedia of Coastal Science*, 452–462. Doi: https://doi.org/10.1007/1-4020-3880-1_144.
- Torsvik T.H. & Cocks L.R.M. 2013. Gondwana from top to base in space and time. *Gondwana Res.* **24**: 999–1030. Doi: <https://doi.org/10.1016/j.gr.2013.06.012>.
- Tulaczyk S., Kamb B., Scherer R.P., Engelhardt H.F. 1998. Sedimentary processes at the base of a West Antarctic ice stream: constraints from textural and compositional properties of subglacial debris. *Journal of Sedimentary Research, Section A. Sedimentary Petrology and Processes*, **68**: 487–496.
- Vail P.R. 1987. Seismic stratigraphy interpretation using sequence stratigraphy. Part I: Seismic stratigraphy interpretation procedure. In: Bally A.W. (ed.). *Atlas of seismic stratigraphy*. p. 1-10. **1**: 125. (Am. Assoc. Petrol. Geol. Stud. Geol. n. 27).
- Vail P.R., Audemard F., Bowman S.A., Eisner P.N., Perez-Cruz C. 1991. The stratigraphic signatures of tectonics, eustasy and sedimentology: an overview. In: Einsele G., Ricken W., Seilacher A. (eds.). *Cycles and events in stratigraphy*. Springer-Verlag, Berlin. 617-659.
- Van der Meer J.J.M. 1993. Microscopic evidence of subglacial deformation. *Quaternary Science Reviews*. **12**: 553-587.
- Van Wagoner J.C., Posamentier H.W., Mitchum R.M., Vail P.R., Sarg J.F., Loutit T.S., Hardenbol, J. 1988. An overview of the fundamentals of sequence stratigraphy and key definitions. In: Wilgus, C.K., Hastings, B.S., Kendall, C.G.St.C., Posamentier, H.W., Ross, C.A., Van Wagoner, J.C. (eds.). *Sea-level changes: an integrated approach*. (SEPM). Houston. 39–45. (Society of Economic Paleontologists and Mineralogists Special Publication. n. **42**).
- Vaz P.T., Resende N.G.A.M., Wanderley Filho J.R., Travassos W.A. 2007. Bacia do Parnaíba. *Boletim de Geociências*, Rio de Janeiro, Petrobrás, **15**(2): 253-263.
- Visser J.N.J. 1991. Self-destructive collapse of the Permo-Carboniferous marine ice sheet in the Karoo Basin: evidence from the southern Karoo. *S. Afr. J. Geol.*, **94**: 255-262.
- Visser J.N.J. 1997. Deglaciation sequences in the Permo-Carboniferous Karoo and Kalahari basins of southern Africa: a tool in the analysis of cyclic glaciomarine basin fills. *Sedimentology*. **44**: 507 - 521. Doi: <https://doi.org/10.1046/j.1365-3091.1997.d01-35.x>.

- Wagreich M., Lein R., Sames B. 2014. Eustasy, its controlling factors, and the limno-eustatic hypothesis - Concepts inspired by Eduard Suess. *Austrian Journal of Earth Sciences*. **107**: 115-131.
- Walker R. G. 1992. Facies, facies models and modern stratigraphic concepts. In: Walker R. G. & James N. P. (eds). *Facies models - response to sea level change*. Ontario, p.1-14. (Geological Association of Canada).
- White W. A .1973. Deep erosion by infracambrian ice sheets. *Geol Soc Am Bull.*, **84**: 1841–1844.
- Whitehouse P. 2018. Glacial isostatic adjustment modelling: historical perspectives, recent advances, and future directions. *Earth Surface Dynamics*, **6**: 401-429. Doi: <https://doi.org/10.5194/esurf-6-401-2018>.
- Winsemann J., Asprion U., Meyer T., Schramm C. 2007. Facies characteristics of Middle Pleistocene (Saalian) ice-margin subaqueous fan and delta deposits, glacial Lake Leine, NW Germany. *Sed. Geol.*, **193**: 105–129.
- Wizevic M.C. 1991. Photomosaics of outcrops: useful photographic techniques. In: Miall A.D. & Tyler N. (eds). *The three-dimensional facies architecture of terrigenous clastic sediments and its implications for hidrocarbon discovery and recovery*. Tulsa, Society for Sedimentary Geology/SEPM. p.22-24.
- Zecchin M. & Catuneanu O. 2013. High-resolution sequence stratigraphy of clastic shelves In: units and bounding surfaces. *Marine and Petroleum Geology*, **39**: 1-25.
- Zecchin M., Octavian C., Rebescu M. 2015. High-resolution sequence stratigraphy of clastic shelves IV: High-latitude settings. *Marine and Petroleum Geology*. **68**: 427-437.
- Zhang T., Kershaw S., Wan Y., Lan G. 2000. Geochimical and facies evidence for palaeoenvironmental change during the Late Ordovician Hirnantian glaciation in South Sichuan Province, China. *Glob. Planet. Change*. **24**: 133-152.